Addis Ababa University

Addis Ababa Institution of Technology

Department of Electrical and Computer Engineering

Neural Network Based Speed Estimation of Induction Motor Using Indirect Field Oriented Control Methods

By

Birhanu Gizaw

A Thesis Submitted to the School of Graduate Studies of Addis Ababa University

In Partial Fulfillment of the Requirements for the Degree of Master of Science

In Electrical Engineering (Control Stream)

Advisor

Dr. Dereje Sheferaw

March,2017

Addis Ababa University

Addis Ababa Institution of Technology

Department of Electrical and Computer Engineering

Neural Network Based Speed Estimation of Induction Motor Using Indirect Field Oriented Control Methods

By

Birhanu Gizaw

Approval by Board of Examiners

_____	_____
Chairman, Dept. Graduate Committee	Signature
Dr. Dereje Sheferaw	_____
Advisor's Name	Advisor Signature
_____	_____
Internal Examiner	Signature
_____	_____
External Examiner	Signature

Declaration

I, the undersigned, declare that this thesis is my original work, has not been presented for a degree in this or any other university, and all sources of materials used for the thesis have been fully acknowledged.

Birhanu Gizaw _____

Name Signature

Place: Addis Ababa, Ethiopia

Date of Submission: March,2017

This thesis has been submitted for examination with my approval as a university advisor.

Dr. Dereje Sheferaw _____

Advisor's Name Signature

Acknowledgment

Next to St. Marry and with Son- The Almighty God, I would like to express my truthful gratefulness to my advisor Dr. Dereje Sheferaw for his continuous support of my thesis, for his patience, motivation, interest, and most importantly, his friendship. His guidance helped me in all time of the research and writing of this thesis.

Beside my advisor, I would like to thank all Friends of Electrical and Computer Engineering Department for their assistance and encouragement throughout my work.

Last but not least, I would like to thank my family for their great support during my study.

Table of Content

List of Figure

List of Abbreviations and Symbols

AC /ac	*Alternating Current*
AI	*Artificial Intelligence*
ANN	*Artificial Neural Network*
DC/dc	*Direct Current*
DTC	*Direct Torque Control*
DTFC	*Direct Torque and Flux Control*
EKF	*Extended Kalman Filer*
ELO	*Extended Lupberger Observer*
ES	*Expert System*
FLC	*Feedback Linear Control*
FOC	*Filed Oriented Control*
FPGA	*Filed Programmable Gate Array*
GA	*Genetic Algorithm*
IM	*Induction Motor*
IVC	*Indirect Vector Control*
LMS	*Least Mean Square*
LQ	*Linear Quadrant*
MATLAB	*Matrix Laboratory*
MRAS	*Model Reference Adaptive Control*
NN	*Neural Network*
PID	*Proportional Integration Derivations*
PLC	*Programming Logic Controller*
rpm	*revolution per minute*
V/Hz	*Voltage/Hertz*
**/ref*	*Reference quantity*
d, q	*Reference Frame (d-axis, q-axis)*
α, β	α *-axis and* β *-axis reference frame*

Abstract

Induction motor is one of the most widely used machines in industrial applications due to its high reliability, relatively low cost, and less maintenance requirements. Vector control of ac machine behaves similar to separately excited dc machine in which the torque and flux are controlled independently. Nevertheless, conventional vector controlled induction motor drive has the disadvantage of required speed sensor and parameter sensitive, unknown variation during operation causes incorrect decoupling of flux and torque which leads to deterioration of drive performance. Sensorless speed control of induction machine has improvement of reducing the system size, cost and high system reliability. The aim of this thesis is to design robust speed estimation of induction motors based on NN by reducing the system components and achieve high dynamic performance. A neural network is an information processing system that is highly interconnected processing element working in unison used as an approach, stator voltage and current used as an input of NN and rotor speed as an output. The performance of the proposed system has investigated through simulations by allowing for system response (at no-load and load condition) and variation of motor parameter such as, variation of stator and rotor resistance, and speed tracking. The error of simulation result between actual and estimated speed have been approximately less than *0.25%* for transient response and *4%* for speed tracking. Lastly, the simulation result is established in *MATLAB/SIMULINK* and the pictures have been draw in *Enterprise Architect* and Microsoft *Visio*.

Chapter One

Introduction

1.1 Background of Induction Motor

In electrical engineering, electrical machine is a general term for electric motors, and electric generators. They are electromechanical energy converters: an electric motor converts electricity to mechanical power while an electric generator converts mechanical power to electricity. Since any given electrical machine can convert power in either direction, any machine can be used as either a generator or a motor. Almost all practical motors and generators convert energy from one to another through the action of a magnetic field, and only machines using magnetic field to perform conversion [1]. Electrical motors in the home run refrigerators, freezers, vacuum cleaners, blenders, air conditioners, fan and many similar appliances. In the workplace motors provide the motive power for almost all tools. Of course, generators are necessary to supply the power used by all these motors.

The induction motor (IM) is widely used in industry because of its advantages such as reliability, efficiency, and low cost in comparison to other motors used in similar application [2]. This is particularly true in industry for which part of work will be applies, where a host of processes require efficient control of speed and high performance torque response. However, an IM constitutes a theoretically challenging control problem, since it is a nonlinear multivariable time varying system and it is subject to unknown external disturbances while its parameters change during operation. The induction motor control system is based on the field oriented control (FOC), the direct torque control (DTC) and many other sensorless control algorithms for induction motors [3] [23].

The induction motor has many advantages:

- The induction motor is rugged, inexpensive and easy to maintain.
- Induction motors range in size from a few watts to values on the order of large watts.
- The speed of an induction motor is nearly constant. The speed typically varies only a few percent going from no load to rated load.

Some disadvantages of the induction motor are:

- The speed is not easily controlled
- The starting current may be five to eight times the full load current
- The lagging power factor is low when the machine is lightly loaded.

1.2 Statement of Problem

The motor control issues are conventionally handled by fixed gain proportional integral (PI) and proportional integral derivation (PID) controllers. However, the fixed gain controllers are very sensitive to parameter variations, load disturbances. Thus, the controller parameters must be continually adapted or tuned.

In induction machines, torque and speed control had implemented by identifying first order system dynamics, which is a very challenging task. It is highly nonlinear with many of its parameters varying with time and with operating conditions. Many conventional induction motor approaches, such as field oriented control (FOC) aim at linearizing the dynamical model. FOC systems have been extensively and successfully applied, but they undergo from sensitivity to parameter variations.

Basically, it is possible to use speed sensor for accessing actual speed information for controlling of induction motor. This speed sensor has its own disadvantage like: extra cost, system configuration and reducing reliability. For solving of these problem, neural network based estimation using FOC has applied to the control of induction motor.

1.3 Objective of Study

General Objective:

The general objective of the thesis is:

- To design robust speed estimation of induction motors based on NN by reducing the system components and achieve high dynamic performance.

Specific Objective:

The specific objective of thesis are:

- To model induction motor based on stationary reference frame
- To train artificial neural network for speed estimation to obtain good dynamic performance.
- To identify PI control of induction motor based on FOC
- To simulate the neural network based speed estimation system on induction motor using MATLAB SIMULINK
- Comparison of the performance of the proposed method with the sensored motor drive.

1.4 Methodology

The research methodology of the thesis involves many of different tasks that has been performed to lead towards completion. The first task is describing the statement of the problem and define the objectives of the research. This is followed by the literature survey where all the theoretical information regarding to speed control of induction motor and neural network have been gathered. Collect the data from different literature survey, text books, journals, and conference paper regarding to neural network estimation based of induction motor. A detail mathematical model of induction motor has discussed. Describe filed oriented control of induction motor.

An ANN was configured for a specific application, speed estimation through a learning process to analysis the dynamic performances. The simulation carried out for MATLAB/Simulink and analysis the performance of Artificial Intelligence (AI) for estimation system. Finally, formulate the conclusion and recommendation of the thesis based on the Simulink result. The flow chart representing of the methodology of the thesis is shown in Figure 1.1.

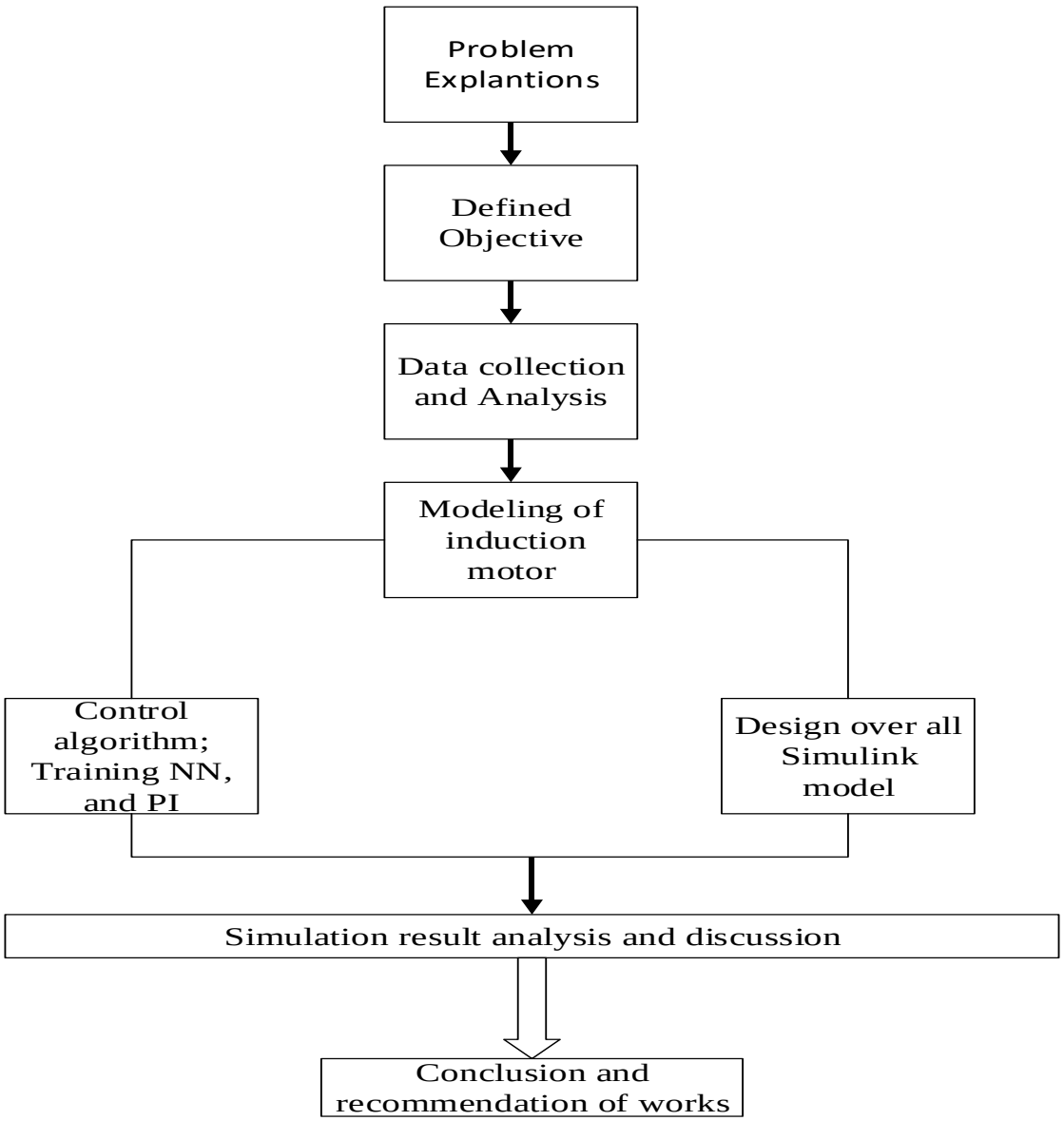

Figure 1-1:General Methodology Flow Chart

The Neural network based speed estimation of induction motor is shown in Fig.1.2. The speed command signal ω_{ref} is compared with estimated value ω_{es} and the error is delivered to the speed controller. As input signals to the ANN speed estimator are stator voltage and stator current. The actual speed ω_m is compared with estimated speed by scope for testing.

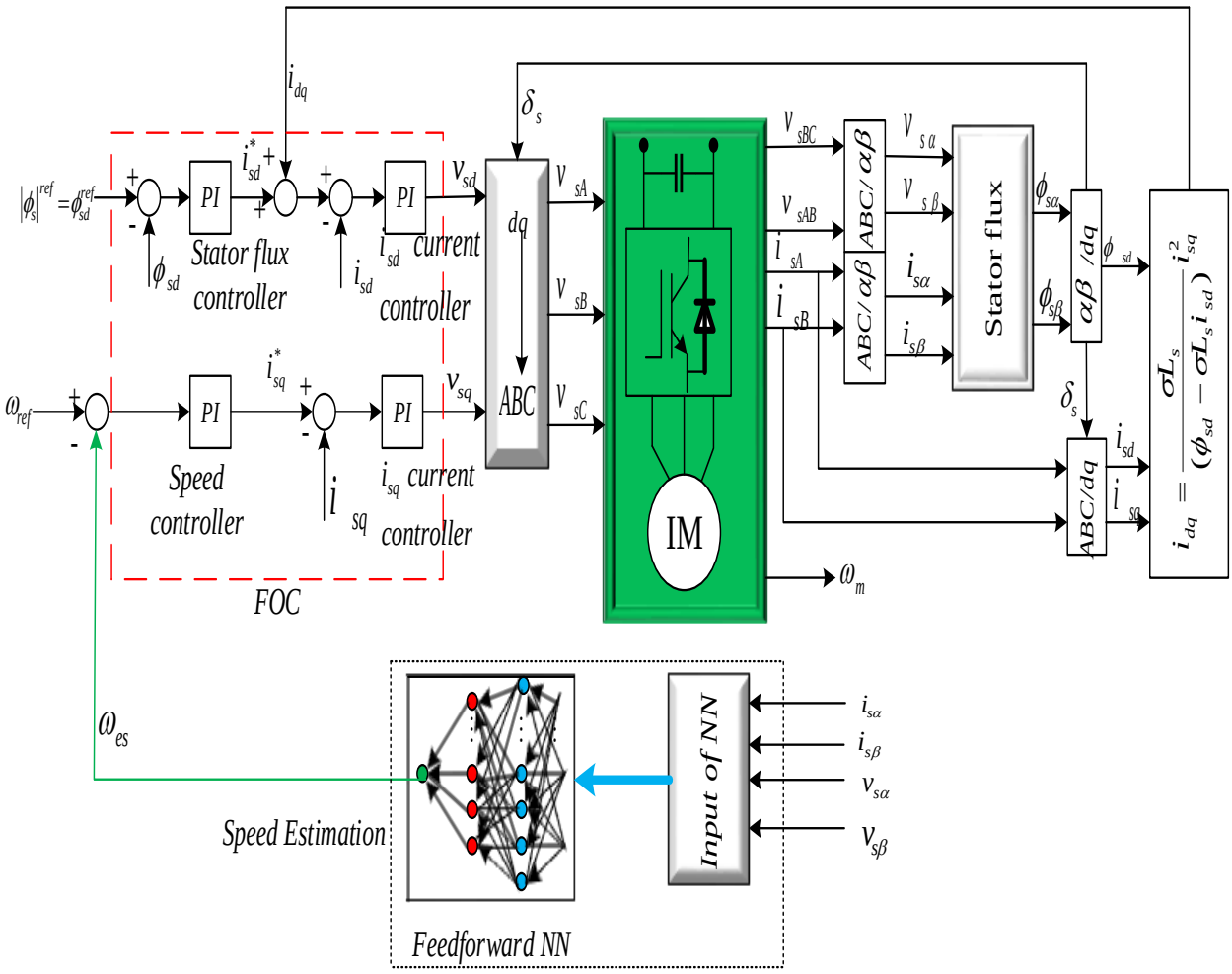

Figure 1-2:General schematic of NN based speed estimation system

1.5 Scope and Limitation

There are different techniques of induction motor speed estimation. For this case, neural network based estimator was carried out high dynamics performance and simulate in MATLAB/SIMUIK. Intending to fulfill the general objective and specific objective outline in detail above the physical scope of the research was bounded to the particularly to neural network and filed oriented control of induction motor.

1.6 Literature Review

Speed control of induction motor drives has been a topic of interest for many years. And different books, and articles have been reported control of electrical machine.

Reference [4] has presented the implementation of intelligent controller and PID for speed control of induction motor has been developed and analyzed. In this paper has discussed the comparison of intelligent controller and PID control induction motor. The challenging and excelling the human brain is one of our long-cherished dreams. Intelligent controllers reflect human thinking, human perception and human way of reasoning. Simulation studies show that the Neural Networks controller provides better results compared to a conventional PI controller. So, Neural Networks controller has an attractive technique when the plant model is complex. The controller scheme needs tuning of the input/output scaling factors which is additional job for the processor which increases the time of response of the system.

Reference [5] has discussed control of induction motor using artificial intelligent. The induction motor drive is a dynamic nonlinear system with uncertainty in the machine parameters. The aim of this study is to improve tracking performance of the induction motor drive. The method for controlling induction motor drives has presented with conventional controller (PI) and artificial neural network controller and the result show in MATLAB/SIMULINK. For this study the dynamic performance of artificial neural network has better than conventional controller (PI). It observed that the speed of the machine remains constant with smart dynamic performance using the neural network controller. Since, most of the investigator proposed multilayer neural network shows high performance and good sensorless control accuracy for the system with field oriented control method [6].

Field oriented control (FOC) theory has the base of special control methods for induction motor drives. With this theory induction motor, can be controlled like a separately excited dc motor. This method enables the control of filed and torque of induction machine independently by manipulating the corresponding oriented quantities. Three speed control techniques, vector, scalar and conventional controller are used to compare the performance of the control system with fuzzy logic controller. The simulation results demonstrate that the

performance of the field oriented control technique with fuzzy logic controller has better, especially with dynamic performance [7]. For this, filed oriented control has improved for applying induction machine with artificial intelligence. Genetic algorithm optimization for tuning different parameters of ANN controller at one time [8]. So, the artificial intelligence gives great opportunity to find out stochastically solution for the problem holding up to high number of indetermination in a minimal time and effort.

All of aforementioned techniques present a good performance, but in term of fast response and robustness against uncertainties including; parametric variations, external disturbance rejection, and difficult model dynamics, the FOC speed control with synchronous current controller have been applied to the improvement of neural network based speed estimation of IM sensorless control.

1.7 Application of the Research

In this work, achieved the application of an artificial neural network for speed estimation of an induction motor based on the overdue samples of stator currents and voltages. The main application of this study has been a normal method of training the neural network, and the identification of speed is based on an integrator free. This structure has increased the performance of the system, especially for the low speeds, variable speed operation and different load.

1.8 Organization of Thesis

The thesis has organized into five chapters. Chapter one presents the introduction, statement of the problem, objectives of the study, the methodology and literature review leading towards the completion of the thesis. The second chapter discusses about modeling of induction motor, Clark and Park transformation, stator and rotor based reference frame model of induction machine. Chapter three presents the control of on induction machine: line voltage control, scalar control, vector control, sensorless control, and the principle of neural network. The simulation results obtained using MATLAB/SIMULINK and discussions of the results are presented in chapter four. The final chapter taking about conclusion and suggestions for future works.

Chapter Two

Induction Machine Modeling

2.1 Introduction

Since the invention of the induction motor by Nikola Tesla in 1886, the use of three phase squirrel cage induction motors has grown extremely in industry. The advantage of using an induction motor comes with its rugged and economic design and reliable performance even in adverse conditions. Induction motors are regularly installed outdoors, exposed to rain and sandstorms, and have been found at the bottom of oil wells [9]. Thus, the induction motor has found widespread use throughout the world. There are two different type of induction motor rotors [1]. One is called a cage rotor, while the other is called a wound rotor. Approximately 60% of electrical energy worldwide passes through the windings of squirrel cage induction motors. This thesis serves to provide a circumstantial to the squirrel cage induction motor.

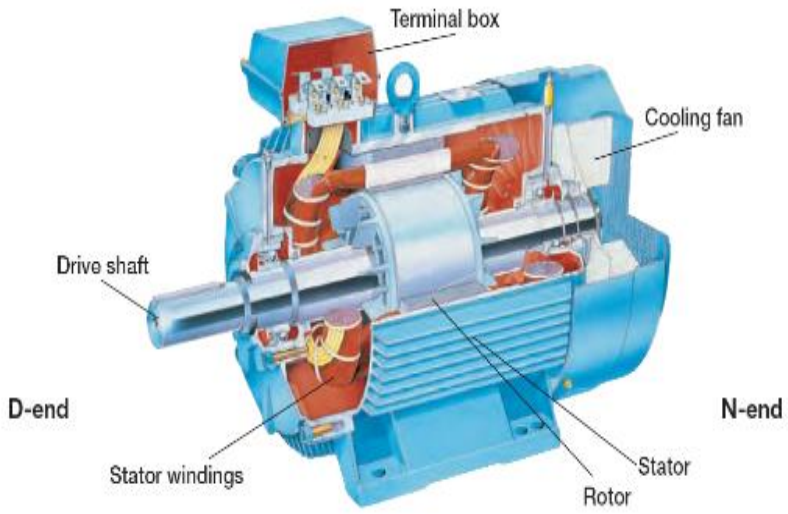

Figure 2-1:Squirrel Cage Induction Motor [20]

2.2 Squirrel Cage Induction Motor

The induction motor works on the principle that electrical power supplied to the stator will produce a rotating magnetic flux through its iron and air gap. This rotating flux, in turn, induces currents in the rotor conductors. There currents interact with the original flux to generate a torque to make the rotor turn. The stator has insulated windings embedded in the inner slots of the iron periphery. The placement and connection of these windings determines the number of electrical poles of the motor. As indicated by his name, the rotor of a squirrel cage induction motor consists of a number of aluminum bars short-circuited on both ends with a pair of end rinds, similar to the configuration of a squirrel cage. As a sinusoidal excitation is applied to the windings of stator, a sinusoidal flux is established in the air gap rotating at a speed given by:

$$N_s = \frac{120 f_s}{P} \tag{2.1}$$

where N_s is the speed in rpm, f_s is the frequency of the applied excitation in Hz, and P is the number of poles. The rotor attempts to turn at this speed, also known as the synchronous speed, but never quote reaches this speed, rotating instead at a speed N_r due to slip. The difference between the source angular frequency (ω_s) and the angular frequency of the rotor electrical speed (ω_r) is termed the angular slip frequency (ω_{sl}) while the ratio of the slip speed to the stator speed is the actual slip (S) [1] [11]. Thus,

$$S = \frac{N_s - N_r}{N_s} = \frac{\omega_s - \omega_r}{\omega_s} = \frac{\omega_{sl}}{\omega_s} \tag{2.2}$$

Note that slip can also be defined in terms of N_r and N_s as shown in equation (2.2) where N_r is the rotor speed in *rpm*. There must always exist some non-zero slip to running unload will often be running at very nearly zero slip.

2.3 Reference Frames

Modelling of induction is the first and essential step for its identification and control [10]. The mathematical model of the machine should on one hand have such a structure to completely describe the characteristics of the machine and on the other hand be convention to use it for implementing estimation algorithms.

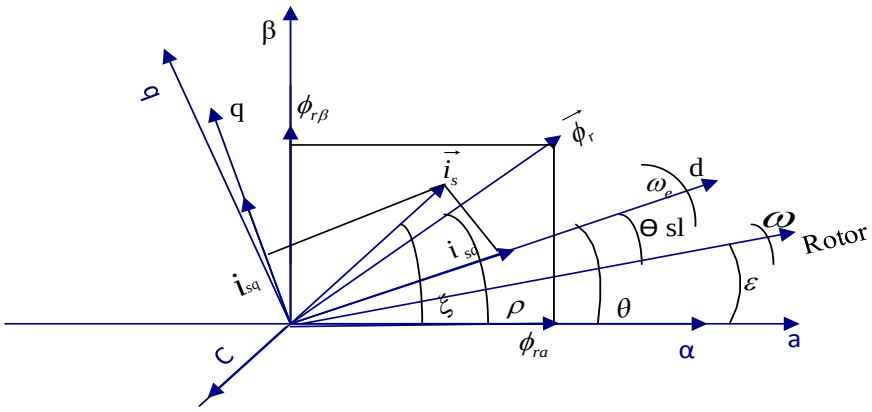

Figure 2-2:Stator Current and Rotor Flux as Space Vector Reference Frame

In the development of an induction machine model, a three-phase machine with symmetrical windings is assumed. Figure 2.2 shows the reference frames and representation of stator current and rotor flux as space vectors. In the figure a, b and c are respectively the axes of the stator windings a, b and c. $\alpha - \beta$ axis is the axis of the fixed stator reference frame, where α has been considered to the coincident with stator winding axis 'a'. *d-q* is an arbitrary reference frame rotating with a synchronous speed.

2.4 Clark Transformation

Regardless of the number of phase, all AC stator are based upon the same premise, the imposition of a rotating magnetic field on the motor of the machine. As the basic operation of these designs are the same, it possible to develop an equivalent two phase model of a three

phase or higher phase AC stator, by which mean a model which would impose the same rotating magnetic field on the rotor. We can then analyze this two-phase model using the analytical techniques and relate the result directly to the actual three phase machine. In order to relate the three-phase machine to its equivalent two phase model, we must be able to transform the three phase electrical variables into their equivalent two phase values [23].

If balanced currents with the same peak values are used and the phase winding of the two design have the same number of turns, the three-phase machine will generate a magnetic field whose magnitude is 3/2 times the magnitude of the two-phase machine due to the combination of the fields generated by the three phases [11]. Hence, when determining the equivalent two phase machine field components from the three phase fields, we must reduce the overall magnitude by a factor of 2/3.

For the three to two phase model transformation or Clarke transformation, we will generalize this relation to all variables in the machine, such as currents, voltages, flux linkages, etc. generally, the Clarke transformation three phase machine is:

$$i_d = \frac{2}{3} i_a - \frac{1}{3} i_b - \frac{1}{3} i_c \tag{2.3}$$

$$i_q = \frac{\sqrt{3}}{3} \left(i_b - i_c \right) \tag{2.4}$$

we will also define a zero-sequence component, which will consist of the average value of the three phase variables:

$$i_0 = \frac{1}{3} (i_a + i_b + i_c) \tag{2.5}$$

we note that in balanced three phase operation, $i_0 = 0$.

The zero-sequence component of the three-phase current does not generate a magnetic field component in the rotor of the machine, as the zero-sequence component of the air gap fields

generated by the three phase cancel one another. The combination of all three variables, direct, quadrature, and zero sequence, are referred to as a *dq0* model.

The transformation from three phase stationary reference frame a-b-c into two phase arbitrary stationary reference frame d-q commonly known as Clarke transformation is given as:

$$\begin{bmatrix} i_{sd} \\ i_{sq} \end{bmatrix} = \frac{2}{3}\begin{bmatrix} \cos(\theta) & \cos(\theta - \frac{2\text{pi}}{3}) & \cos(\theta + \frac{2\text{pi}}{3}) \\ \sin(\theta) & \sin(\theta - \frac{2\text{pi}}{3}) & \sin(\theta + \frac{2\text{pi}}{3}) \end{bmatrix}\begin{bmatrix} i_{sa} \\ i_{sb} \\ i_{sc} \end{bmatrix} \tag{2.6}$$

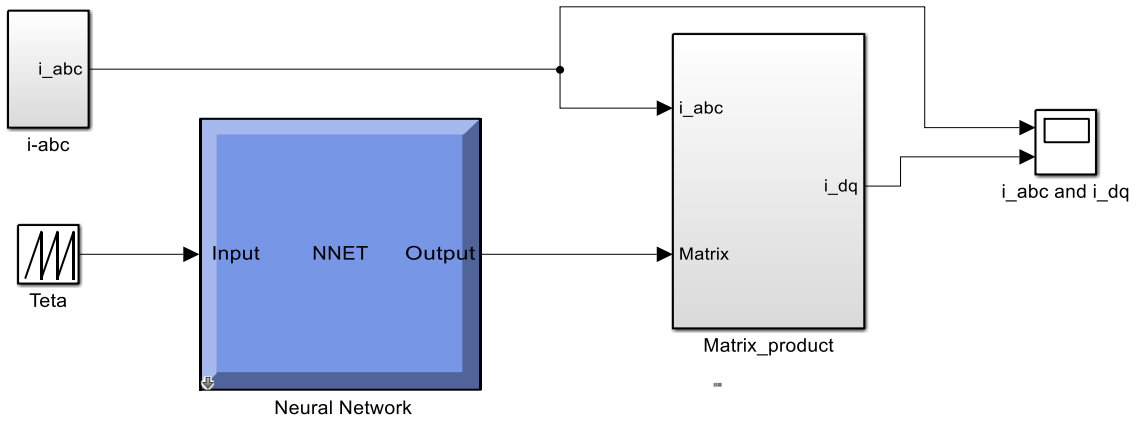

Figure 2-3:MATLAB Model of Equation (2.6) Based on NN

In the model, the 'i_{abc}' block yields three phase current [i_a, i_b, i_c] with frequency 60 Hz , magnitude 1 A and the value of θ (0,2π) with a period of 2 sec. The neural network (four neurons in the first layer and with activation transfer function is *tansig* and six neurons in output layer with activation function is *pure liner*) blocks yields Clark's transformation matrix. The matrix product blocks implements product operation of [i_a, i_b, i_c] and the Clark's transformation matrix to give i_d and i_q. After running of the model the first scope displays the three phase current [i_a, i_b, i_c], and the second scope displays current [i_d i_q] of rotating

d-q reference frame. This implies that how much true of the transformation of *d-q* reference frame based on NN. The simulation results are shown in figure 2.4 shown below:

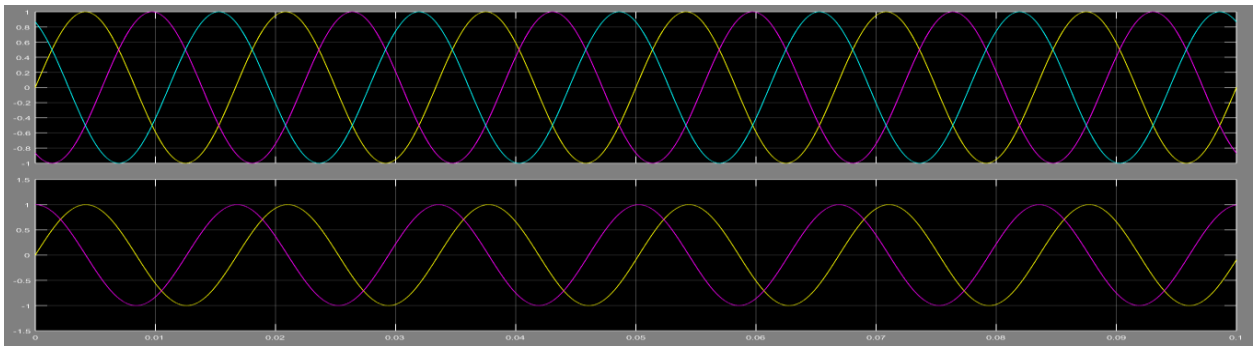

Figure 2-4:Three phase current (i_a, i_b, i_c) and ($i_d \ \ i_q$) output of d-q reference frame

The reverse transformation from two phase to three phase or reverse Clark transformation is given below:

$$\begin{bmatrix} i_{sa} \\ i_{sb} \\ i_{sc} \end{bmatrix} = \frac{3}{2} \begin{bmatrix} \cos(\theta) & \sin(\theta) \\ \cos(\theta - \frac{2\text{pi}}{3}) & \sin(\theta - \frac{2\text{pi}}{3}) \\ \cos(\theta + \frac{2\text{pi}}{3}) & \sin(\theta + \frac{2\text{pi}}{3}) \end{bmatrix} \begin{bmatrix} i_{sd} \\ i_{sq} \end{bmatrix} \tag{2.7}$$

we have considered current as the variable. The voltage and flux linkages can also be transformed by similar equations. In addition to this when d-axis aligned with the a-axis then the transformation simplifies as like Equation (2.3-2.4) which means Clark and park transformation are the same:

$$\begin{bmatrix} i_{sd} \\ i_{sq} \end{bmatrix} = \begin{bmatrix} i_{s\alpha} \\ i_{s\beta} \end{bmatrix} = \frac{2}{3} \begin{bmatrix} 1 & -0.5 & -0.5 \\ 0 & -\frac{\sqrt{3}}{2} & \frac{\sqrt{3}}{2} \end{bmatrix} \begin{bmatrix} i_{sa} \\ i_{sb} \\ i_{sc} \end{bmatrix} \tag{2.8}$$

And the inverse of Clark transformation:

$$\begin{bmatrix} i_{sa} \\ i_{sb} \\ i_{sc} \end{bmatrix} = \frac{3}{2}\begin{bmatrix} 1 & 0 \\ -0.5 & -\frac{\sqrt{3}}{2} \\ -0.5 & \frac{\sqrt{3}}{2} \end{bmatrix}\begin{bmatrix} i_{sa} \\ i_{s\beta} \end{bmatrix} \tag{2.9}$$

2.5 Park Transformation

The conversion from the a-b-c frame to the fixed frame $\alpha - \beta$ gives value in a stationary reference frame fixed to the stator. It is often useful to model the machine in an alternative reference frame, usually rotating at synchronous speed. The transformation from the stationary frame to any frame d-q rotating at an angular speed $\omega_{e,}$ also known as the park transformation is given as:

$$\begin{bmatrix} i_{sd} \\ i_{sq} \end{bmatrix} = \begin{bmatrix} \cos\theta & \sin\theta \\ -\sin\theta & \cos\theta \end{bmatrix}\begin{bmatrix} i_{sa} \\ i_{s\beta} \end{bmatrix} \tag{2.10}$$

where θ is, the angle between the synchronously rotating reference frame d-axis and the stationary frame a- axis. The reverse transformation from the synchronous frame to stationary frame or revers park transformation is given by [12[13]]:

$$\begin{bmatrix} i_{s\alpha} \\ i_{s\beta} \end{bmatrix} = \begin{bmatrix} \cos\theta & -\sin\theta \\ \sin\theta & \cos\theta \end{bmatrix}\begin{bmatrix} i_{sd} \\ i_{sq} \end{bmatrix} \tag{2.11}$$

2.6 Space Vector Representation of Induction Machine

Although the complex vector approach to writing the machine, equations results in a compact form, the essential sinusoidal coupling between the stator and rotor circuits with rotor position remain [14]. Space vector representation of induction machine is given in this section. The machine model is represented in a rotating as well as fixed reference frames.

2.6.1 Induction Machine Model in Rotating Reference Frame

The induction motor model in an arbitrary reference frame d-q, rotating with a synchronous speed ω_e using complex vector notations given as [2] [15].

$$\overrightarrow{v_s}e^{-i\theta} = R_s\overrightarrow{i_s}e^{-i\theta} + \frac{d\overrightarrow{\phi_s}e^{-i\theta}}{dt} + i\omega_e\overrightarrow{\phi_s}e^{-i\theta} \quad (2.12)$$

$$0 = R_r\overrightarrow{i_r}e^{i(\varepsilon-\theta)} + \frac{d\overrightarrow{\phi_r}e^{i(\varepsilon-\theta)}}{dt} + i(\omega_e - \omega_r)\overrightarrow{\phi_r}e^{i(\varepsilon-\theta)} \quad (2.13)$$

where $\overrightarrow{v_s}$, $\overrightarrow{i_s}$ and $\overrightarrow{\phi_s}$ are respectively the stator voltage, current and flux vectors in stator reference frame: $\overrightarrow{i_r}$ and $\overrightarrow{\phi_r}$ are the rotor current and flux in rotor reference frame respectively. The stator and rotor fluxes given below:

$$\overrightarrow{\phi_s}e^{-i\theta} = L_s\overrightarrow{i_s}e^{-i\theta} + L_m\overrightarrow{i_r}e^{i(\varepsilon-\theta)} \quad (2.14)$$

$$\overrightarrow{\phi_r}e^{i(\varepsilon-\theta)} = L_r\overrightarrow{i_r}e^{i(\varepsilon-\theta)} + L_m\overrightarrow{i_s}e^{-i\theta} \quad (2.15)$$

The electromechanical equation is given by:

$$J\frac{d\omega_r}{dt} = pT_{em} - pT_l - F\omega_r \quad (2.16)$$

where J is load inertia, F is viscous friction, T_{em} is electromechanically torque, T_l is load torque, p is number of pair of poles and ωr is rotor speed of the motor.

The electromagnetic torque is given by:

$$T_{em} = \frac{3}{2}pL_m\Im\left[\overrightarrow{i_s}e^{-i\theta}(\overrightarrow{i_r}e^{i(\varepsilon-\theta)})^*\right] \quad (2.17)$$

The imaginary part of the bracket is equivalent to the vector products of the stator current and the conjugated of rotor current. The equation of electromagnetic torque can also describe as:

$$T_{em} = \frac{3}{2}p\left\{(\overrightarrow{\phi_s}e^{-i\theta})\times(\overrightarrow{i_s}e^{-i\theta})\right\} = \frac{3}{2}p\frac{L_m}{L_r}\left\{(\overrightarrow{\phi_r}e^{-i(\varepsilon-\theta)})\times(\overrightarrow{i_s}e^{-i\theta})\right\} \quad (2.18)$$

2.6.2 Induction Machine Model in Stator Reference Frame

When induction machine model in fixed stationary reference frame, the value of θ and ω_e to be zero we can model stationary reference frame given as [17]:

$$\overrightarrow{v_s} = R_s \overrightarrow{i_s} + \frac{d\overrightarrow{\phi}}{dt} \tag{2.19}$$

$$0 = R_r \overrightarrow{i_r} e^{i\varepsilon} + \frac{d\overrightarrow{\phi_r} e^{i\varepsilon}}{dt} - i\omega_r \overrightarrow{\phi_r} e^{i\varepsilon} \tag{2.20}$$

2.7 Two Phase Induction Machine Model

The first mathematical model for the dynamic analysis of the induction machine was based on the two axis reference frame, developed initially by park in 1929 for the synchronous machine. Using the symmetric configuration of the induction machine, have elaborated the space complex vector theory, and obtained a model for the steady state analysis of the machine [12] [16]. Both theories are used for modelling the three-phase induction machine the following assumptions are made when a complete equations system to describe the model of induction machine [21].

- Geometrical and electrical machine configuration is symmetrical
- Space harmonics of the stator and rotor magnetic flux are negligible
- Stator and rotor windings are distributed in space and replaced by an equivalent concentrated winding
- Core loss and skin effect are negligible
- Currents and voltage are sinusoidal
- Balanced operating conditions

Three phase induction machines are supplied by three phase symmetrical voltage. The windings of the motors are arranged within the stator and mutually shifted by 120 electrical degrees. The machines operate with circular magnetic fields [18]. Two phase representation of three phase induction machine is very useful in designing control and estimation

algorithms. The rotating and fixed reference frame are discussed for the next topics, but more information is concerned with the system chose to the later one.

2.7.1 Two Phase Machine Model in Rotating Reference Frame

Considering the model of the machine in a d-q frame with rotor flow and the stator current like variables of state:

$$\frac{d}{dt}\begin{bmatrix} i_{sd} \\ i_{sq} \\ \phi_{rd} \\ \phi_{rq} \end{bmatrix} = A(\omega_e, \omega_r)\begin{bmatrix} i_{sd} \\ i_{sq} \\ \phi_{rd} \\ \phi_{rq} \end{bmatrix} + B\begin{bmatrix} v_{sd} \\ v_{sq} \end{bmatrix} \qquad (2.21)$$

The induction machine equivalent circuits in synchronously rotating d-q axis reference frame are shown in Figure 2.5 [16][19] where ω_e is the synchronous frequency of the reference frame, so for the stationary frame model it's equal to zero.

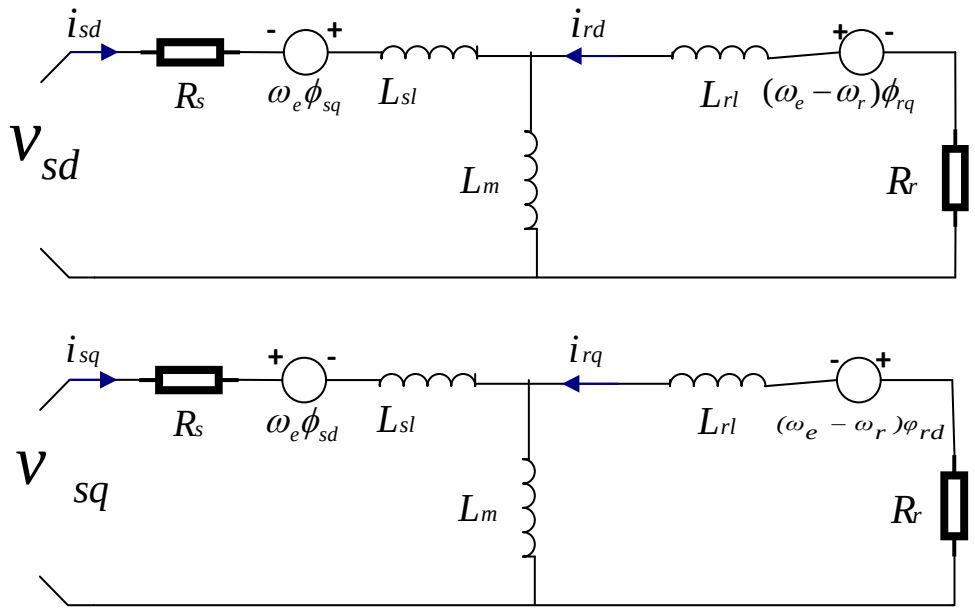

Figure 2-5:D-Q Axis Equivalent Circuit [19]

The expanding using the equations for the variables current and flux linkage and adding the variable of speed, the model of the machine in arbitrary fame could be presented by in which σ is the coefficient of dispersion, ω_e is the synchronous frequency of the reference frame, p

is the number of the pole pair. *F* is the damping coefficient and *J* is the total rotor inertia is given below [30]:

$$\frac{d}{dt}\begin{bmatrix} i_{sd} \\ i_{sq} \\ \phi_{rd} \\ \phi_{rq} \end{bmatrix} = \begin{bmatrix} -\{\frac{Rs}{\sigma Ls}+\frac{Rr(1-\sigma)}{\sigma Lr}\} & \omega_e & \frac{RrLm}{\sigma LsLr^2} & \frac{Lm\omega_r}{\sigma LsLr} \\ -\omega_e & -\{\frac{Rs}{\sigma Ls}+\frac{Rr(1-\sigma)}{\sigma Lr}\} & -\frac{Lm\omega_r}{\sigma LsLr} & \frac{RrLm}{\sigma LsLr^2} \\ \frac{RrLm}{Lr} & 0 & -\frac{Rr}{Lr} & (\omega_e-\omega_r) \\ 0 & \frac{RrLm}{Lr} & -(\omega_e-\omega_r) & -\frac{Rr}{Lr} \end{bmatrix}\begin{bmatrix} i_{sd} \\ i_{sq} \\ \phi_{rd} \\ \phi_{rq} \end{bmatrix} + \frac{1}{\sigma L_s}\begin{bmatrix} v_{sd} \\ v_{sq} \\ 0 \\ 0 \end{bmatrix} \tag{2.22}$$

$$\frac{d\omega_r}{dt} = \frac{\mathrm{P}^2 L_m}{JL_r}(i_{sq}\phi_{rd} - i_{sd}\phi_{rq}) - \frac{F}{J}\omega_r - \frac{P}{J}T_l \tag{2.23}$$

In rotor frame, ω_e is equal to ω_r, then the model of induction motor is given by:

$$\frac{d}{dt}\begin{bmatrix} i_{sd} \\ i_{sq} \\ \phi_{rd} \\ \phi_{rq} \end{bmatrix} = \begin{bmatrix} -\{\frac{Rs}{\sigma Ls}+\frac{Rr(1-\sigma)}{\sigma Lr}\} & \omega_r & \frac{RrLm}{\sigma LsLr^2} & \frac{Lm\omega_r}{\sigma LsLr} \\ -\omega_r & -\{\frac{Rs}{\sigma Ls}+\frac{Rr(1-\sigma)}{\sigma Lr}\} & -\frac{Lm\omega r}{\sigma LsLr} & \frac{RrLm}{\sigma LsLr^2} \\ \frac{RrLm}{Lr} & 0 & -\frac{Rr}{Lr} & 0 \\ 0 & \frac{RrLm}{Lr} & 0 & -\frac{Rr}{Lr} \end{bmatrix}\begin{bmatrix} i_{sd} \\ i_{sq} \\ \phi_{rd} \\ \phi_{rq} \end{bmatrix} + \frac{1}{\sigma L_s}\begin{bmatrix} v_{sd} \\ v_{sq} \\ 0 \\ 0 \end{bmatrix} \tag{2.24}$$

2.7.2 Two Phase Machine Model in Stator Reference Frame

Two phase stationary frame $\alpha - \beta$, assume that the machine are linear magnetic circuits and balanced operation conditions, then the phase voltage equation given as:

$$v_{s\alpha} = R_s i_{s\alpha} + \frac{d\phi_{s\alpha}}{dt} \tag{2.25}$$

$$v_{s\beta} = R_s i_{s\beta} + \frac{d\phi_{s\beta}}{dt} \tag{2.26}$$

$$v_{ra} = 0 = R_r i_{r\alpha} + \omega_r \phi_{r\beta} + \frac{d\phi_{r\alpha}}{dt} \tag{2.27}$$

$$v_{r\beta} = 0 = R_r i_{r\beta} - \omega_r \phi_{r\alpha} + \frac{d\phi_{r\beta}}{dt} \tag{2.28}$$

where R_r and R_s are rotor and stator resistance, $(v_{sa}, v_{s\beta})$ and $\{v_{ra}, v_{r\beta}\}$ are stator and rotor voltage , $\{i_{sa}, i_{s\beta}\}$ and $(i_{sa}, i_{s\beta})$ are stator and rotor current, ϕ_r and ϕ_s are the linkage flux, ω_r is electrical rotor speed of the machine.

The flux equations become:

$$\begin{bmatrix} \phi_{s\alpha} \\ \phi_{s\beta} \\ \phi_{r\alpha} \\ \phi_{r\beta} \end{bmatrix} = \begin{bmatrix} L_s & L_m & 0 & 0 \\ 0 & 0 & L_s & L_m \\ L_m & L_r & 0 & 0 \\ 0 & 0 & L_m & L_r \end{bmatrix} \begin{bmatrix} i_{s\alpha} \\ i_{r\alpha} \\ i_{s\beta} \\ i_{r\beta} \end{bmatrix} \tag{2.29-32}$$

Where $\{Ls\ , Lr\ Lm\}$ the stator and rotor inductance and the later one is mutual inductance.

The electromagnetic torque and speed are:

$$T_{em} = \frac{3}{2} P(\phi_{s\alpha} i_{s\beta} - \phi_{s\beta} i_{s\alpha}) \tag{2.33}$$

$$J\frac{d\omega_m}{dt} = T_{em} - T_l - F\omega_m \tag{2.34}$$

$$\omega_r = p\omega_m \tag{2.35}$$

Where ω_m is mechanical speed of rotor, ω_r electrical rotor speed and *p* a number of pair of poles: From equation (2.29 and 2.31) the current in the axis of α, i_{sa} and i_{ra} are:

$$i_{sa} = \frac{Lr}{L_s L_r - L_m^2}\phi_{s\alpha} - \frac{L_m}{L_s L_r - L_m^2}\phi_{r\alpha} \tag{2.36}$$

$$i_{ra} = \frac{L_s}{L_s L_r - L_m^2}\phi_{r\alpha} - \frac{L_m}{L_s L_r - L_m^2}\phi_{s\alpha} \tag{2.37}$$

Similarly, from equation (2.30 and 2.32) the current in the axis of β:

$$i_{s\beta} = \frac{L_r}{L_s L_r - L_m^2}\phi_{s\beta} - \frac{L_m}{L_s L_r - L_m^2}\phi_{r\beta} \tag{2.38}$$

$$i_{r\beta} = \frac{L_s}{L_s L_r - L_m^2}\phi_{r\beta} - \frac{L_m}{L_s L_r - L_m^2}\phi_{s\beta} \tag{2.39}$$

Using equation (2.36 and 2.37) calculate the derivation of stator flux, equation (2.25) and (2.26) becomes:

$$\frac{d\phi_{s\alpha}}{dt} = v_{s\alpha} - \frac{R_s L_r}{L_s L_r - L_m^2}\phi_{s\alpha} + \frac{R_s L_m}{L_s L_r - L_m^2}\phi_{r\alpha} \tag{2.40}$$

$$\frac{d\phi_{s\beta}}{dt} = v_{s\beta} - \frac{R_s L_r}{L_s L_r - L_m^2}\phi_{s\beta} + \frac{R_s L_m}{L_s L_r - L_m^2}\phi_{r\beta} \tag{2.41}$$

Similarly, the derivation of rotor flux drive from equation (2.27) and (2.28) by using equation (2.37) and (2.39) it gives:

$$\frac{d\phi_{r\alpha}}{dt} = \frac{R_r L_m}{L_s L_r - L_m^2}\phi_{s\alpha} - \frac{R_r L_s}{L_s L_r - L_m^2}\phi_{r\alpha} - P\omega_m\phi_{r\beta} \tag{2.42}$$

$$\frac{d\phi_{r\beta}}{dt} = \frac{R_r L_m}{L_s L_r - L_m^2}\phi_{s\beta} - \frac{R_r L_s}{L_s L_r - L_m^2}\phi_{r\beta} + P\omega_m \phi_{r\alpha} \tag{2.43}$$

Finally, the electromagnetic torque from equation (2.34) by substitute equation (2.36) and (2.38) and the rotor speed gives as below respectively:

$$T_{em} = \frac{3}{2}.P\frac{L_m}{L_s L_r - L_m^2}(\phi_{s\beta}\phi_{r\alpha} - \phi_{r\beta}\phi_{s\alpha}) \tag{2.44}$$

$$J\frac{d\omega_m}{dt} = \frac{3}{2}.P\frac{L_m}{L_s L_r - L_m^2}(\phi_{s\beta}\phi_{r\alpha} - \phi_{r\beta}\phi_{s\alpha}) - T_l \tag{2.45}$$

The angel of stator flux and magnitude is calculated from $\tan\delta_s = \frac{\phi_{s\beta}}{\phi_{s\alpha}}$ and $|\phi_s| = \sqrt{\phi_{s\alpha}^2 + \phi_{s\beta}^2}$ respectively.

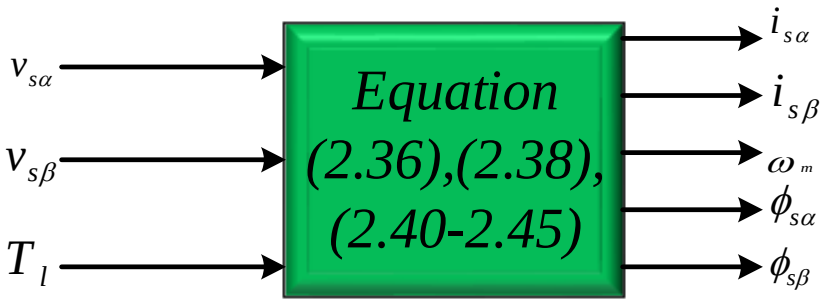

Figure 2-6: Stator reference frame of IM model

Equation (2.25 and 2.26) shows that the accuracy of the estimated stator flux depends on the accuracy of the estimated resistance. Usually, the stator resistance can be measured with accuracy and it is relatively easy to adapt its slow variation with temperature. Therefore, it is reasonable to assume that the stator flux can be estimated accurately.

Chapter Three

Control of Induction Machine

3.1 Induction Machine Control Techniques

An induction machine is essentially a constant speed machine, if connected to a constant voltage and constant frequency power supply. In this case the operating speed is very closed to the synchronous speed and changes in the torque makes small changes in the speed. It is suitable for use in constant speed drive systems, while in variable speed uses the controllers are more complicated than traditional dc motor controllers. The induction motor can be described by a fifth order nonlinear differential equation with two inputs and state variables are available for measurement. There are various methods for controlling the speed of an induction motor which are shortly discussed in the following. Figure 3.1 show that the general schematic of induction machine control system consists of the controller, sensors, inverter, and the induction motor.

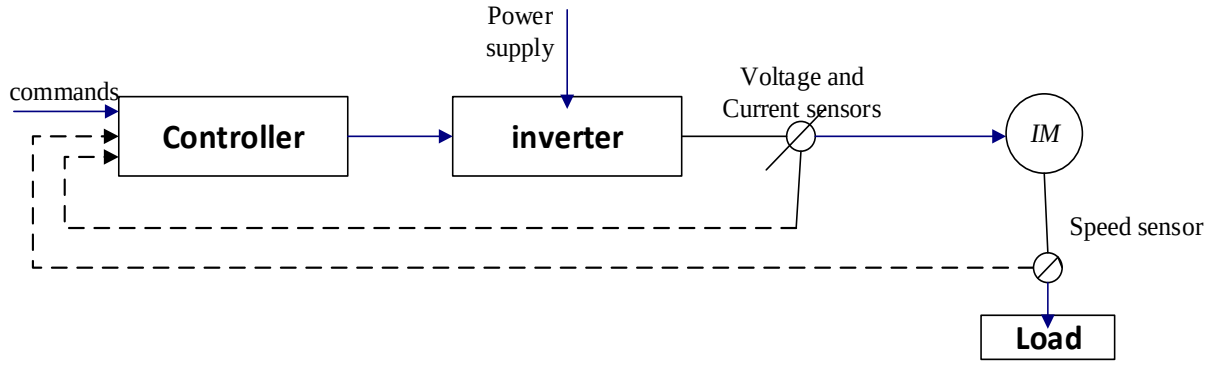

Figure 3-1:Induction Machine Control System

3.2 Line Voltage Control

This method is useful for small motors with fan loads. The torque developed in an induction machine is proportional to square of the terminal voltage [22] [2]. In the Figure 3.2 firing the thyristors at a firing angle, provides a terminal voltage for the motor.

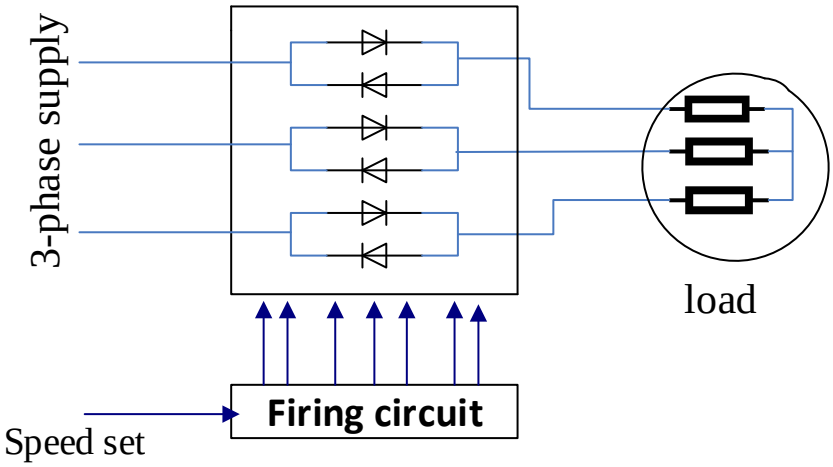

Figure 3-2:Open Loop Voltage Controller

The closed loop controller has given accurate speed control of desired value. In such a controller, the difference between the set speed and the motor speed would correct the firing angle of the thyristors. The voltage controllers are simple, although inefficient for all purposes.

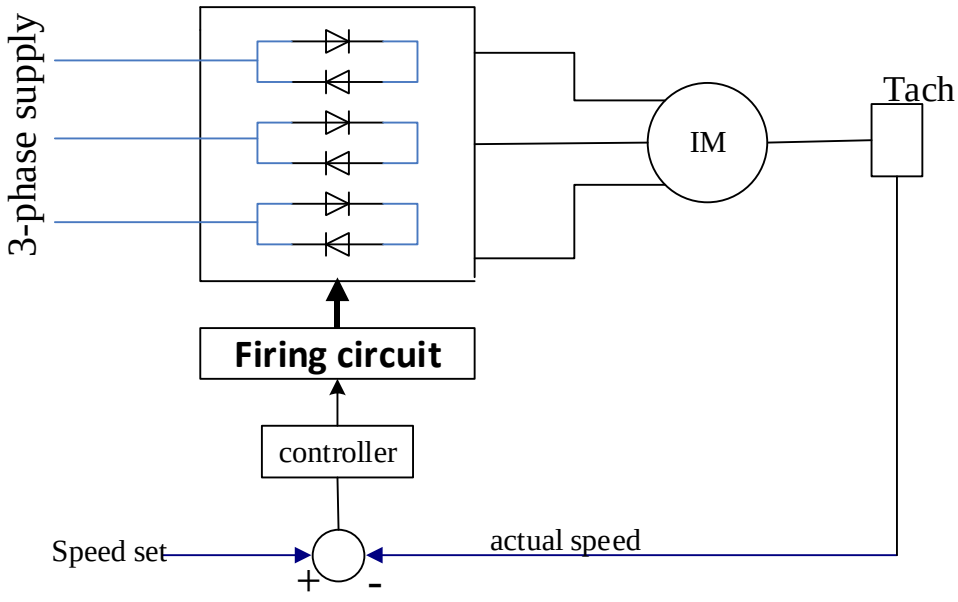

Figure 3-3:Closed Loop Voltage Controller

3.3 Closed loop control

Industrial drives mostly operate as closed loop feedback systems. In this topic discus about constant v/f operation and constant slip frequency.

3.3.1 Constant V/F Operation

The block diagram of a constant volt/hertz operation in which the difference between the set speed (n^*) and the actual speed (n_r) represents the slip speed, hence the angular slip frequency. This slip angular frequency (n_{sl}^*) is added to actual speed (n_r) to generate the stator angular frequency (n_e). The function generator provides a signal such as a voltage obtained to keep the *volts/ hertz* as a constant.

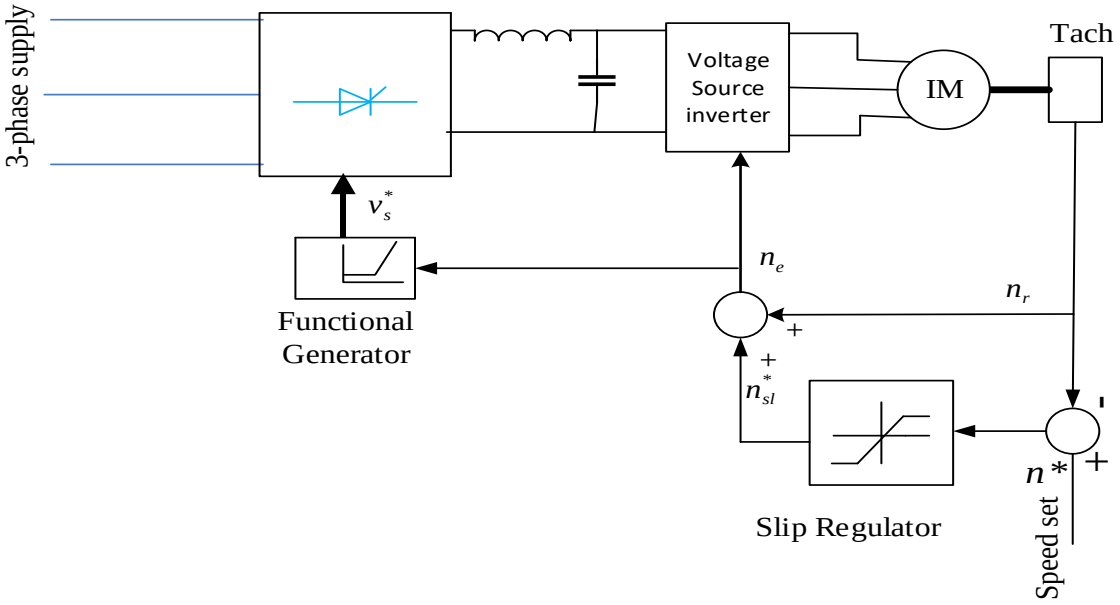

Figure 3-4:Closed Loop Speed Control and Constant V/F Operation[23]

3.3.2 Constant Slip Frequency

Another possibility for a simple speed control system is to keep the slip frequency constant and control the speed by controlling the current and hence the magnitude flux of the motor, using a current source inverter as is shown in the block diagram of Figure 3.5. In this scheme the torque command is given to the drive as either a current command or a slip command. The current/slip relationship is then utilized to calculate the slip or current command.

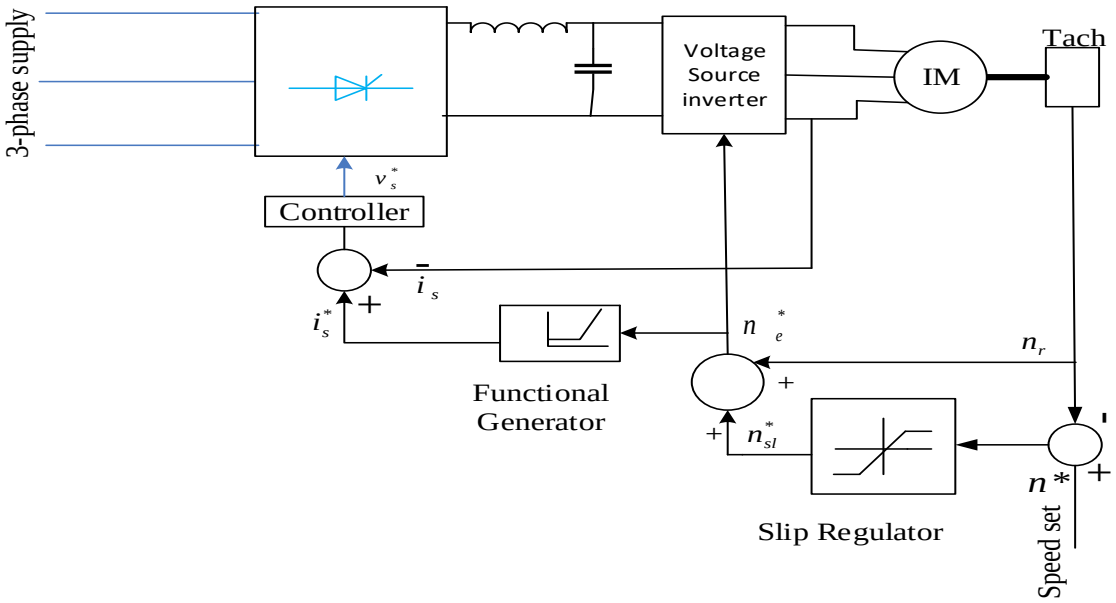

Figure 3-5: Closed Loop Speed Control with Slip Frequency[2]

The constant slip regulation scheme offers better dynamic performance than the volts/hertz scheme with the disadvantage of requiring both speed and current transducers.

3.4 Scalar and Vector Control

3.4.1 Scalar Control

Scalar control is based on the steady state model of the machine. The control is due to the magnitude variation of the control variables only and disregards the coupling effect in the machine. For example, the voltage of a machine can be controlled to control the flux, and frequency or slip can be controlled to control torque. However, flux and torque are also

function of frequency and voltage respectively. This method is simple and robust but, it has poor dynamic performance. Under steady state condition the machine equation is:

$$\overrightarrow{v_s} = R_s \overrightarrow{i_s} + i\omega_e \overrightarrow{\phi_s} \tag{3.1}$$

$$0 = R_r \overrightarrow{i_r} + i(\omega_e - \omega_r)\overrightarrow{\phi_r} \tag{3.2}$$

From equation (3.2) we have

$$\overrightarrow{\phi_r} = -i\frac{R_r}{\omega_{sl}}\overrightarrow{i_r} \tag{3.3}$$

$$\text{or, } \overrightarrow{i_r} = -i\frac{\omega_{sl}}{R_r}\overrightarrow{\phi_r} \tag{3.4}$$

From equation (2.15)

$$\overrightarrow{i_s}e^{-i\theta} = \frac{\overrightarrow{\phi_r}e^{i(\varepsilon-\theta)}}{L_m} - \frac{L_r}{L_m}\overrightarrow{i_r}e^{i(\varepsilon-\theta)} \tag{3.5}$$

The electromagnetic torque is given by:

$$T_{em} = \frac{3pL_m}{2L_r}(\overrightarrow{\phi_r}e^{i(\varepsilon-\theta)}) \times (\overrightarrow{i_s}e^{-i\theta}) \tag{3.6}$$

Substituting the stator current (3.5) in equation (3.6):

$$T_{em} = \frac{3p}{2}(\overrightarrow{\phi_r}e^{i(\varepsilon-\theta)}) \times (\overrightarrow{i_r}e^{i(\varepsilon-\theta)}) \tag{3.7}$$

Replacing the rotor current with that in equation (3.7)

$$T_{em} = \frac{3p\omega_{sl}}{2R_r}\phi_r^{\,2} \tag{3.8}$$

Equation (3.8) shows that at constant flux the torque is proportional to the slip, or at constant slip the electromagnetic torque is proportional to square of the flux.

3.4.2 Vector Control

The scalar control is somewhat simple to implement, but the inherent coupling effect (both torque and flux are functions of voltage or current and frequency) gives sluggish response and system is disposed to instability because of a high order system effects [20]. For example, if the torque is increased by increasing the slip (the frequency), the flux tends to decrease. The flux variation in such system is always sluggish. The decrease in flux is then compensated by the sluggish flux control loop feeding in additional voltage. This temporary dipping of flux reduces the torque sensitivity with slip and lengthens response time. Therefore, high performance induction motor drives use vector or filed oriented control (FOC) or direct torque and flux control (DTFC) or feedback linearized control (FLC) [25].

Vector control is a very widely used control method for high performance induction motor drive applications. It implies independent (decoupled) control of flux and torque components of stator current through a coordinated change in supply voltage amplitude, phase and frequency. The FOC consists of controlling the stator current represented by a vector control is based on projections which transform a three-phase time and speed dependent system into a two co-ordinate (d-q coordinate) time invariant system [40]. These projections lead to a structure like that of a dc machine control. This requires information regarding the magnitude and position of rotor flux vector. In the induction motor magnetizing current is analogous to the main field flux of the dc machine and is controlled by i_{sd} is analogous the armature current of the dc machine and it can be rapidly varied by an appropriate change in stator current to give a fast response to a sudden torque demand. It also controls the angular velocity of rotor flux vector. In steady state operation with sinusoidal currents, the stator current vector and magnetizing current vector in synchronism. Hence i_{sd} and i_{sq} are constant dc quantities and a steady torque is developed.

i) Indirect Vector Control

As the flux vector is rotating simultaneously with the chosen frame (d, q) it's clear that the q-axis rotor flux is zero, therefore

$$\overline{\phi_r} = \phi_{rd} + j\phi_{rq} = \phi_{rd} \tag{3.9}$$

and the voltage equation becomes as

$$0 = R_r i_{rd} + \frac{d\phi_{rd}}{dt} \tag{3.10}$$

Rearranging the flux equation for induction machines to give the direct axis rotor current in terms of the rotor flux and stator current from equation

$$i_{rd} = \frac{\phi_{rd} - L_m i_{sd}}{L_r} \tag{3.11}$$

From the two equations (3.10,3.11)

$$\frac{d\phi_{rd}}{dt} + \frac{R_r}{L_r}\phi_{rd} = \frac{R_r L_M}{L_r} i_{sd} \tag{3.12}$$

Which shows the rotor flux magnitude is related to the direct axis stator current by a first order differential equation, so can be controlled by controlling the direct axis stator current.

In the steady states the rotor flux is directly proportional to the stator axis current as

$$\phi_{rd} = L_m i_{sd} \tag{3.13}$$

The phase of reference system such that the rotor flux is entirely in d-axis the equation ϕ_{rq} is equal to zero, therefore

$$i_{rq} = -\frac{L_m}{L_r} i_{sq} \tag{3.14}$$

On the other hand, voltage equation for q- axis is given as

$$0 = R_r i_{rq} + (\omega_e - \omega_r)\phi_{rd} \tag{3.15}$$

Slip equation (2.2) then results

$$\omega_{sl} = -\frac{R_r}{\phi_{rd}} i_{rq} \tag{3.16}$$

Using the equation of (3.14) then equation (3.16) give as

$$\omega_{sl} = \frac{R_r L_m}{\phi_{rd} L_r} i_{sq} \tag{3.17}$$

The torque equation of induction motor in arbitrary frame:

$$T_e = p\frac{L_m \phi_r i_{sq}}{L_r} \tag{3.18}$$

The indirect vector control can be implemented as:

$$i_{sd}^* = \frac{\phi_r}{L_m} \tag{3.19}$$

$$i_{sq}^* = \frac{L_r}{PL_m}\frac{T_e}{\phi_r} \tag{3.20}$$

$$\omega_{sl}^* = \frac{L_m}{\tau_r}\frac{i_{sq}^*}{\phi_r} \tag{3.21}$$

In the equations above the quantities are commanded or estimated in drive control are denoted by asterisk (*). The time constant τ_r is obtained from

$$\tau_r = \frac{L_r}{R_r} \tag{3.22}$$

The angle θ_s which determines the rotor flux angle is calculated by:

$$\omega_e = \omega_r + \omega_{sl} \tag{3.23}$$

$$\theta_s = \int \omega_e dt \tag{3.24}$$

Substitution equation (3.23) and (3.21) in to (3.24) gives as:

$$\theta_s^* = \int (\omega_r + \frac{R_r L_m i_{sq}^*}{L_r \phi_r^*}) dt \tag{3.25}$$

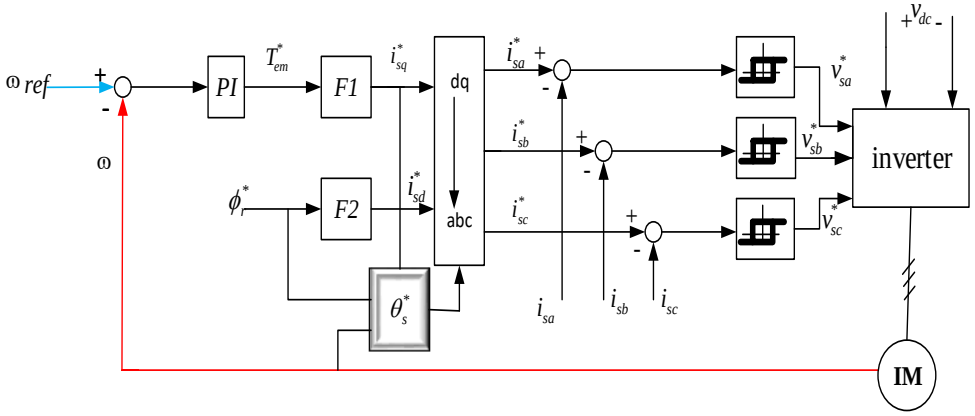

Figure 3-6: Indirect Vector Control Block Diagram

The of *F1* and *F2* are presented by the equations (3.20) and (3.19) respectively. In indirect FOC the rotor flux angle is generated in feedforward manner. Since this method relies on the knowledge of the machine parameters such as L_m and τ_r the real values of which may be changing of the machine in operating condition so care should be given during to take the effects of parameter variations.

The speed control of the induction motor has achieved using a proportional integral (PI) regulator. The design of PI speed controller is disused below. The block diagram of speed control loop is shown in Figure 3.7:

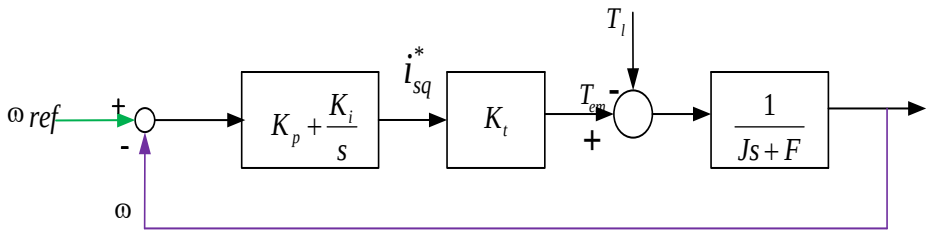

Figure 3-7:Speed Control Block Diagram

From figure

$$T_{em} = K_t i_{sq}^* \tag{3.26}$$

$$i_{sq}^* = \frac{2L_r T_{em}}{3PL_m \phi_r^*} \tag{3.27}$$

$$\phi_r^* = L_m i_{sd}^* \tag{3.28}$$

From equation (3.26-3.28) K_t is given by:

$$K_t = \left(\frac{3PL_m^2}{2L_r}\right) i_{sd}^* \tag{3.29}$$

Closed loop transfer function [24] with respect to the reference input is

$$\frac{\omega}{\omega^*} = \frac{K_i K_t}{Js^2 + (F + K_p K_t)s + K_i K_t} = \frac{\omega_n^2}{s^2 + 2\xi\omega_n s + \omega_n^2} \tag{3.30}$$

Where $\xi = \frac{F + K_p K_t}{2\sqrt{JK_i K_t}}$ and $\omega_n = \sqrt{\frac{K_i K_t}{J}}$

Then, for a unit step input response

$$\omega = \omega^* \frac{\omega_n^2}{s^2 + 2\xi\omega_n s + \omega_n^2} = \frac{1}{s}\frac{\omega_n^2}{s^2 + 2\xi\omega_n s + \omega_n^2} = \frac{1}{s}\frac{\omega_n^2}{(s + p_1)(s + p_2)} \tag{3.31}$$

To obtain a fast response without overshoot, the should be critically damped and stable: $\xi = 1$ and $p_1 = p_2 = \omega_n$: then, the above equation becomes

$$\omega = \frac{1}{s}\frac{\omega_n^2}{(s+\omega_n)^2} = \frac{1}{s} - \frac{\omega_n}{(s+\omega_n)^2} - \frac{1}{(s+\omega_n)} \tag{3.32}$$

The invers of Laplace transform

$$\omega(t) = 1 - \omega_n t e^{-\omega_n t} - e^{-\omega_n t} \tag{3.33}$$

From the solution of the above nonlinear equation we obtain the value of proper frequency using which parameters of the controller can be computed from the equation given below:

$$\begin{cases} 1 = \dfrac{F + K_p K_t}{2\sqrt{JK_i K_t}} \\ \omega_n = \sqrt{\dfrac{K_i K_t}{J}} \end{cases} \tag{3.34}$$

ii) Stator Flux- Oriented Vector Control

The rotor flux oriented system with rotor flux estimated from the terminal quantities has some limitation on the performance due to detuning effects. A major cause of detuning is the variation in the leakage inductance which is used in the flux estimation. The flux estimator can be described by the following equations [42]:

$$\vec{\phi_s} = \int (\vec{v_s} - R_s \vec{i_s}) dt \tag{3.35}$$

$$\vec{\phi_r} = \frac{L_r}{L_m}(\vec{\phi_s} - \sigma L_s \vec{i_s}) \tag{3.36}$$

Where, $\vec{\phi_s}$ is the estimated stator flux vector , $\vec{\phi_r}$ is the estimated rotor flux vector and $\sigma = 1 - \frac{L_m^2}{L_s L_r}$. From (3.35) shows that the accuracy of the estimated stator flux depends on

the accuracy of the estimated stator resistance. Usually, the stator resistance can be measured with accuracy and it is relatively easy to adapt its slow variations with temperature.

On the other hand, (3.36) shows that estimation of rotor flux requires the knowledge of inductances of the machine, especially the leakage inductance. The conventional no load and locked rotor tests do not give the correct value of machine inductances due to closed rotor slots.

To obtain the machine equations in the stator flux reference frame, the q components of the stator flux to be zero. The resultant equations are follows (see appendix b):

$$0 = (1+\sigma T_r p)L_s i_{sq} - \omega_{sl} T_r (\phi_{sd} - \sigma L_s i_{sd}) \tag{3.37}$$

$$0 = (1+\sigma T_r p)L_s i_{sd} - (1+T_r p)\phi_{sd} - \omega_{sl} T_r \sigma L_s i_{sq} \tag{3.38}$$

From (3.37) an expression to determine the slip frequency is:

$$\omega_{sl} = \frac{(1+\sigma T_r p)L_s i_{sq}}{T_r(\phi_{sd} - \sigma L_s i_{sd})} \tag{3.39}$$

In order to decouple ϕ_{sd} from i_{sq}, it is required that:

$$\phi_{sd} = \frac{(1+\sigma T_r p)L_s}{(1+T_r p)}\left(i_{sd} - \frac{\sigma T_r \omega_{sl}}{(1+\sigma T_r p)} i_{sq}\right) \tag{3.40}$$

$$\text{From this, } i_{dq} = \frac{\sigma T_r \omega_{sl}}{(1+\sigma T_r p)} i_{sq} \tag{3.41}$$

Substituting ω_{sl} in to (3.41)

$$i_{dq} = \frac{\sigma L_s}{(\phi_{sd} - \sigma L_s i_{sd})} i_{sq}^2 \tag{3.42}$$

Where, $p = \frac{d}{dt}$ denotes the differential operator and $T_r = \frac{L_r}{R_r}$ is the rotor time constant

From (3.42) and (3.39) describe the decuple which, properly tuned generate a correct i_{sd} for a given i_{sq} so that ϕ_{sd} is not altered.

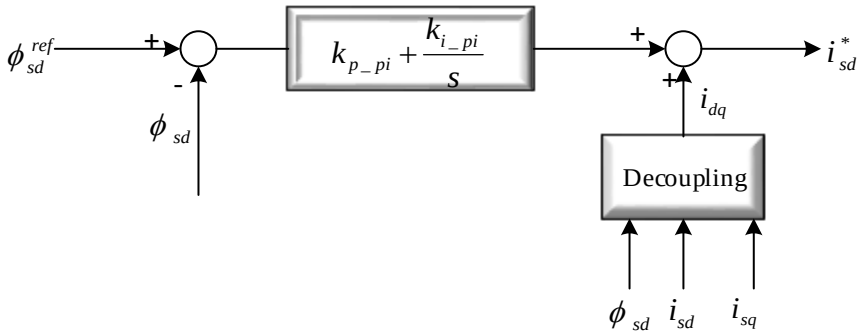

Figure 3-8: feedforward decoupling signal injection

Tune the i_{sd} and i_{sq} loops in Figure 1.2 one at a time. Note that the currents are perpendicular but do not have an orientation with rotor flux and neglect mutual inductance in Figure (2.5). From the principle of circuit analysis: Figure3-9 shows the i_{sq} loop, where k_n is voltage gain ,and $\frac{1}{R+LS}$ is the transient equivalent circuit transfer function. This is similar to i_{sd} .

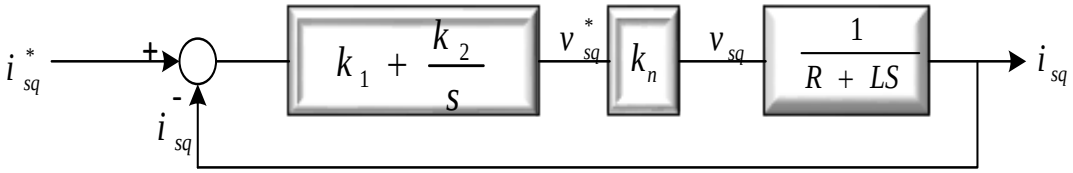

Figure 3-9:stator current loop with P-I control

where $R = R_s + R_r$ and $L = L_{ls} + L_{lr}$, $L_s = L_{ls} + L_m$, $L_r = L_{lr} + L_m$

3.5 Sensor-Less Vector Control of Induction Motor Drive

Ongoing the study has concentrated on the elimination of the speed sensor at the machine shaft without deteriorating the dynamic performance of the drive control system. Speed estimation is an issue of interest with induction motor drives where the mechanical speed of

the rotor is generally different from the speed of the revolving magnetic field. The advantage of speed sensor-less induction motor drives are reduced hardware complexity and lower cost, reduced size of the drive machine, elimination of the sensor cable, better noise immunity, increased reliability and less maintenance requirements. Operation in hostile environments mostly requires a motor without speed sensor [26].

A variety of different solutions for sensor less as drive have been proposed in the past few years. The v/f control principle adjusts a constant V/Hz ratio of the stator voltage by feedforward control. It serves to maintain the magnetic flux in the machine at a desired level. Its simplicity satisfies only moderate dynamic requirements. High dynamic performance is achieved by field orientation, also called vector control. The stator currents are injected at a well-defined phase angle with respect to the spatial orientation of the rotating magnetic field, thus overcoming the complex dynamic properties of the induction motor.

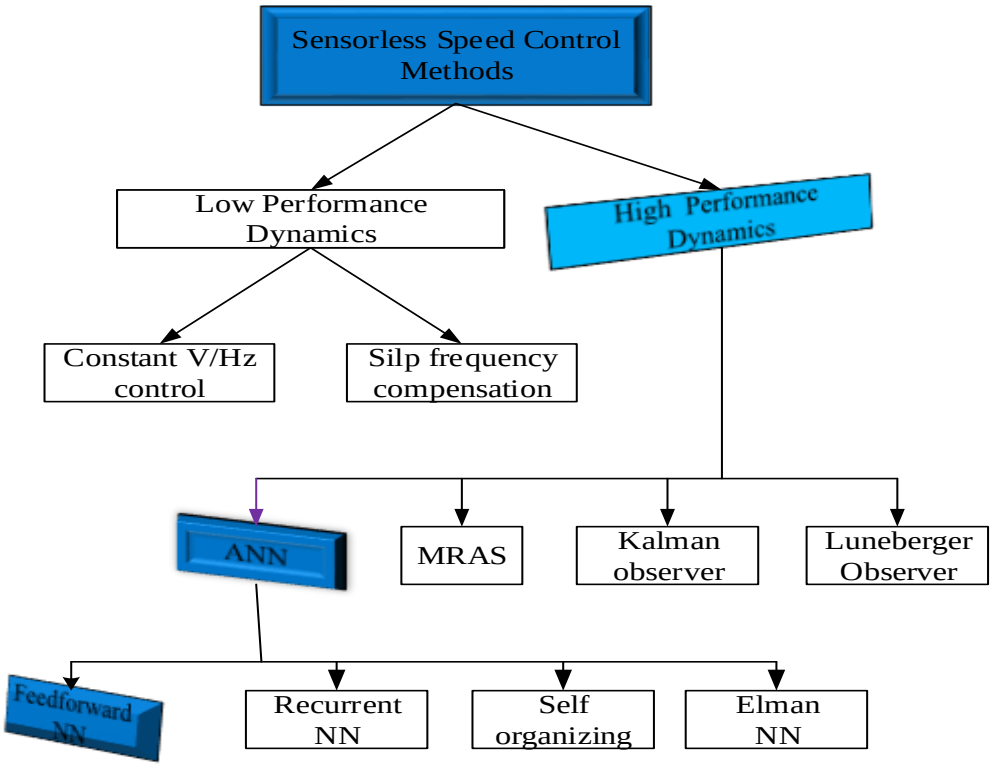

Figure 3-10: Methods of Sensor-less Speed Control

There are various methods of models and algorithms used for speed estimation. Their efficacy depends mostly on the accuracy of parameters identification. Some examples are: Model reference adaptive system, extended Kalman filter, luenberger observers and artificial neural network based estimator.

3.6. Speed Estimation Techniques

3.6.1 Model Reference Adaptive Systems

The method model reference adaptive systems estimated in working out two models one of reference and the command adjustable one for the estimate of two components of stator flux starting from the measurement of the currents and voltages. The estimated speed is obtained by cancelling the difference between stator flux of the adjustable model of reference and that while using the theory of hyper stability to obtain the adaptive mechanism [27] [28].

The main problem in this strategy is that the flux based MRAS require pure integration of sensed variables which leads to problems with initial conditions and drift. To avoid these problems, the pure integration must be replaced with a high gain low pass filter. This replacement causes the instability of identification at low speed, which results to weak performance of speed sensor less vector at low speed [33].

3.6.2 Extended Kalman Filter Observers

Extended Kalman filters is employed to estimate the motor state variable by on using the measurements of stator voltages and currents. During the estimation procedure, these signals are not filter. The accuracy of the speed estimation depends on the motor parameter variations and the accuracy of measured voltage and currents. The EKF is a recursive optimum stochastic state estimator of non-linear dynamic system in real time by using noisy monitored signals that are disturbed by random noise [29-31].

The main design steps for a speed sensor less induction motor drive implementation using the discretized algorithm are:

- Selection of the time domain induction machine model
- Discretization of the machine model

- Determination of the noise and state covariance matrices
- Implementation of the discretized EKF algorithm
- Tuning of the covariance matrices

The main advantage of EKF is the robustness; no comprehensive parameter sensitivity study is in the literature. However, the problems of stator and rotor resistance estimation are addressed, as in the sensitivity of the EKF to rotor time constant is consider [30]. This shows the dependence of the speed estimator on the rotor time constant/ slip relationship like the MRAS. On the other hand, the drawback of EKF can be considered the complexity of the algorithm.

3.6.3 Extended Luenberger observers

The theory of observers started with the works of Luenberger in 1964, so that observers are very often called Luenberger observers. According to Luenberger, any system drive by the output of the given system can serve as an observer for that system [32]. Two main techniques are available for observer design.

The first one is used for the full order observer design and produces an observer that the same dimension as the original system. The second technique exploits the knowledge of some state space variables available through the output algebraic equations (system measurements) so that a reduced order observer is constructed only for estimated state space variables that are not directly obtained from the system measurements.

For the other hand, ELO is based on the determination of the proportionality coefficient between the eigenvalues of the motor and the eigenvalues of the luenberger observer based on an algorithm which ensures the bounded input –bounded output stability of the ELO observer at very low speed both in motor and in regenerating mode running [34]. The comparison of ELO with the EKF shows that similar performance of though the estimation of speed [36].

3.7 Artificial Neural Networks

The artificial intelligence (AI) techniques, such as expert system (ES), artificial neural network (ANN), and genetic algorithm (GA) have recently been applied widely in power electronics and motor drives. The goal of AI is to plant human or natural intelligence in a computer so that can think intelligently like a human being. A system with embedded computational intelligence is often defined as an intelligent system that has learning, self-organizing or self-adapting capability [35]. The cerebral of human brain is said to contain around 100 billion nerve cells or biological neurons, which are interconnected to from a biological neural network. The memory and intelligence of the human brain and the corresponding thinking process are generated by the action of this neural network. An ANN tends to emulate the biological nervous system of the human brain in a very limited way by an electronic circuit or computer program [2]. Many concepts inspired from the behavior of a neuron in biological nervous systems are used in neural network computing (brain like computations). A neural network is an information processing system that is intensely parallel. These specifications make it to be considered a robust estimation method while a nonlinear function is present, and the parameters are not exactly known. The ability of this technique in addressing the problems whose solution have not been explicitly formulated has proven in different areas. Therefore, AI techniques are now being extensively used in industrial process control, image processing, diagnostics, medicine, space technology, and information management system.

From the beginning of 1990s, the neural network technology captivated the attention of a large segment of scientific community. The realization of state estimation problems with helps of control theory methods is relatively simple for linear systems. But in the case of nonlinear systems, like electrical drives, the numbers of difficulties occur in the field of the algorithms synthesis and their practical realizations [37]. For this reason, the ANN are especially attractive in this case because of their possibilities of different nonlinearities approximations and adjustment of designed structure on the base of the non-measurable variables of electrical drives system with the help of the ANN can be performed by the neural modelling.

3.7.1 Application

An artificial neural network is an information processing paradigm that is inspired by the way biological nervous systems, such as brain, process information. The key element of this paradigm is the novel structure of the information processing system. It is composed of large number of highly interconnected processing elements (neurons) working in unison to solve specific problems. Basically, the most applications of neural networks fall into the following categories;

- Prediction: use input values to predict some output in future
- Classification: use input patterns to determine the classification
- Data association: similar to classification, but it also recognizes data that contains errors.
- Data conceptualization: analyze the inputs so that grouping relationships can be inferred
- Data filtering: smooth an input signal, or noise reduction
- Process modeling and control: creating a neural network model for physical plant then using that model to determine the best control setting for the plant

3.7.2 Structure of Neural Network

The structure of biological neural system is the original inspiration for neural networks, which have been developed as generalization of the mathematical models of human cognition or neural biology.

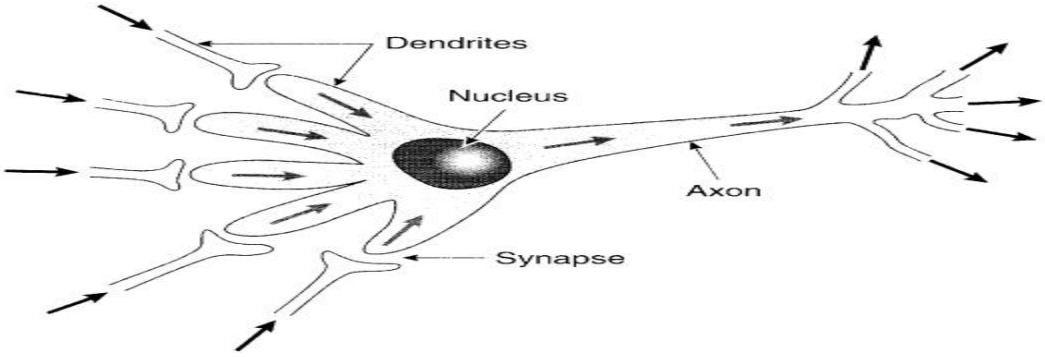

Figure 3-11:Structure of Biological Neuron [35]

A neuron with a single input and no bias is depicted in Figure 3.12 (a). The input is p transmitted through a connection that multiplies its strength by weight w to form the product $w \times p$. Here the weighted input $w \times p$ is the only argument of the transfer function F, which produces the output of a. The neuron on the figure 3.12(b) has a bias b, which is an additional input to the transfer function F. The bias can be viewed as simply being added to the product $w \times p$ or as shifting the F by an amount b. The bias much like a weight, except that it has a constant input of one. The transfer function net input is the sum of the weighted input $w \times p$ and the bias b. This sum is the argument of the transfer function. That means w and b are both adjustable parameters of the neuron.

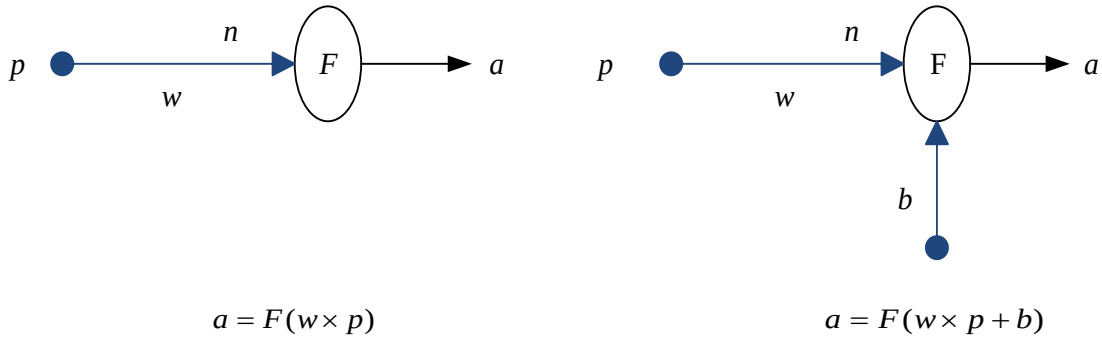

$a = F(w \times p)$ $\qquad$ $a = F(w \times p + b)$

Figure 3-12: a neuron (a) without bias (b) with bias

The transfer function F is typically a step function or a sigmoid function. Typically, a neuron with or without bias has several weighted inputs, where the weights are established during training. Four of the most commonly used neuron transfer functions, commonly called nonlinearities are shown in figures 3.13(a)-(d).

The hard limit transfer function shown in Figure (a) limits the output of the neuron to either 0 or 1. It is often used to create neurons that make decisions such as classification.

The linear transfer function shown in Figure (b) has an output equal to its input plus the bias. Neurons with this transfer function can be used in linear approximations.

The sigmoid transfer functions shown in Figures (c)) and (d) soft limits; the input (which may have any value between plus and minus infinity) in to the range of 0 to 1 or -1 to 1. It is used to in back propagation networks., because they are differentiable.

(a) Hard-limit with bias

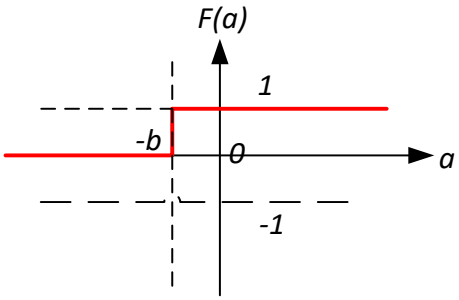

$$F(a)=\begin{cases}1 & if \quad a \geq -b \\ 0 & otherwise\end{cases}$$

(b) Linear with bias

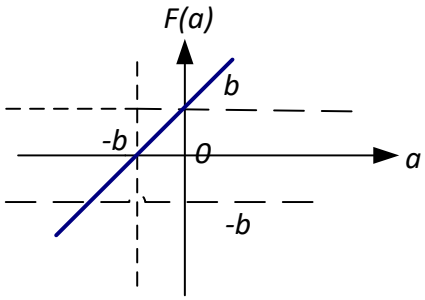

$$F(a)=a+b$$

(c) Sigmoidal

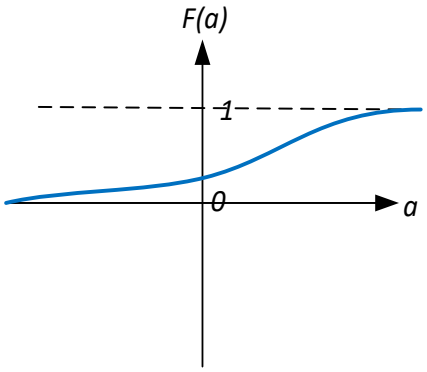

$$F(a)=\frac{1}{1+e^{-a}}$$

(d) Hyperbolic tan

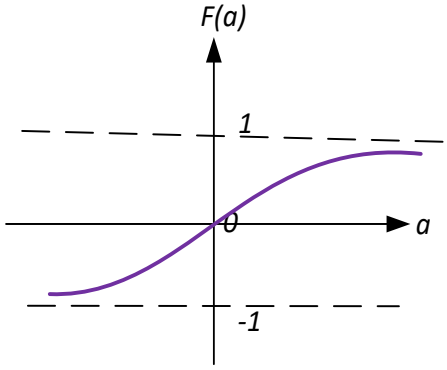

$$F(s)=\frac{e^{a}-e^{-a}}{e^{a}+e^{-a}}$$

Figure 3-13:Activation Function of Artificial Neuron

A single neuron with R inputs is shown in Figure 3.14. Here the individual inputs $P(j)$, weighted by elements $W(i, j)$ of the matrix W are summed to form the weighted inputs to the transfer function F of the i^{th} neuron. The neuron has a bias b and an output a. The transfer function net input is the sum of the weighted inputs $W(i, j)P(j)$ and the bias b. This sum is the argument of the transfer function.

The array of weights $W(i.j)$ and the array of inputs $P(j)$ can be represented as a row vector W and a column vector P as shown below.

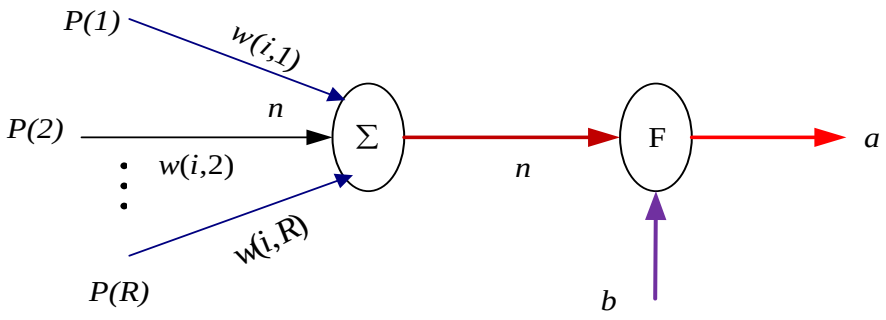

$$a = F(W \times P + b)$$

Figure 3-14: A number of input neuron with bias.

$$W = [W(i,1) \quad W(i,2) \quad \ldots \quad W(i.R)] \quad P = \begin{bmatrix} P(1) \\ P(2) \\ . \\ P(R) \end{bmatrix} \tag{3.43}$$

A one layer network with R inputs and S neurons is shown in Figure 3.15. In this case, each element of the input vector P is connected to each neuron input through the weight matrix W. Each of the S neurons have a summer and the summer of outputs form an S element vector N. The transfer function net input is the sum of its appropriate weighted inputs $W(i, j)P(j)$ and bias $B(i)$. Such sum are the arguments of the transfer functions. Finally, the neuron layer outputs from a column vector A, which is computed as:

$$A = F(W \times P + B) \tag{3.44}$$

It is common for the number of inputs to a layer to be different from the number of neurons (i.e. $R \neq S$). A layer is not constrained to have the number of inputs equal to the numbers of its neurons.

The input vector elements enter the network through the weight matrix W.

$$W = \begin{bmatrix} W(1,1) & W(1,2) & \cdots & W(1,R) \\ W(2,1) & W(2,2) & \cdots & W(2,R) \\ \vdots & \vdots & & \vdots \\ W(S,1) & W(S,1) & \cdots & W(S,R) \end{bmatrix} \tag{3.45}$$

The row indices on the elements of matrix W indicate the destination neuron of the weight and the column indices indicate which source is the input for that weight. For example, the index $W(1,2)$ represents the strength (i.e. weight) of the signal from the second source to the first neuron.

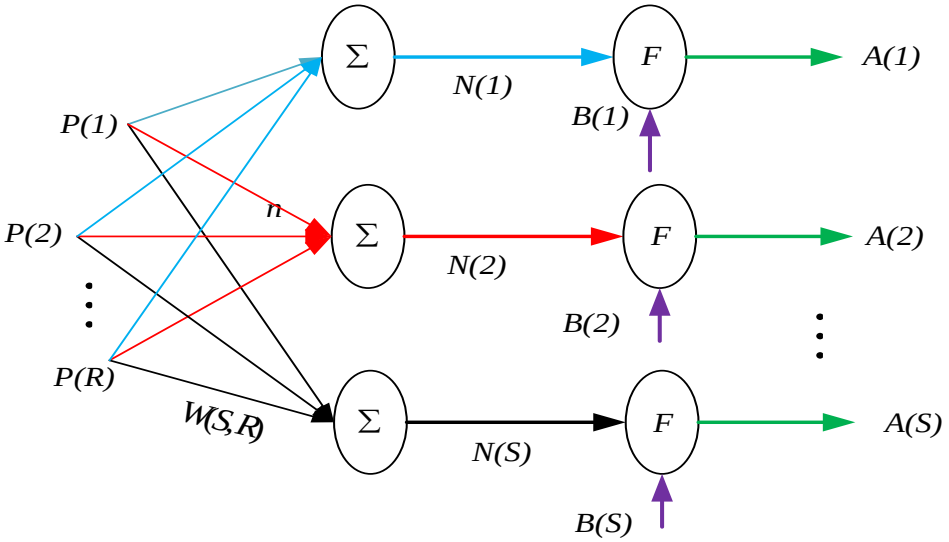

Figure 3-15:Single Layer Network

A network can have several layers. Each layer has a weight matrix W, a bias vector B, a weighted input N and an output vector A. The layers of a multilayer network paly different

roles. The layer whose output becomes the network is called the output layer. The layer whose input is the network input is called the input layer. All other layers are called hidden layers. A three-layer network is shown in Figure (3.16). It has one output layer (layer 3), one input layer (layer 1) and one hidden layer (layer 2).

The network shows in Figure 3.16 has R inputs, $S1$neurons in the first layer, $S2$ neurons in the second layer, etc. It is common for different layers to have different numbers of neurons. A constant input one is fed to the biases for each neuron. In this thesis use three layers, ten neurons in the first layer, five neurons in the second layers, and one neurons in third layers. The last layers determine the final output from neural network training.

The output of each intermediate layer are the inputs to the following layer. Thus layer 2 can be analyzed as a one layer network with $R = S1$ inputs, $S = S1$ neurons and an S by R weight matrix $W = W2$. The input to layers 2 is $P = A1$, the output is $A = A2$. Now that all the vectors and the matrices of layer 2 are identified we can treat it as a single layer network on its own. This approach can be taken with any layer of network.

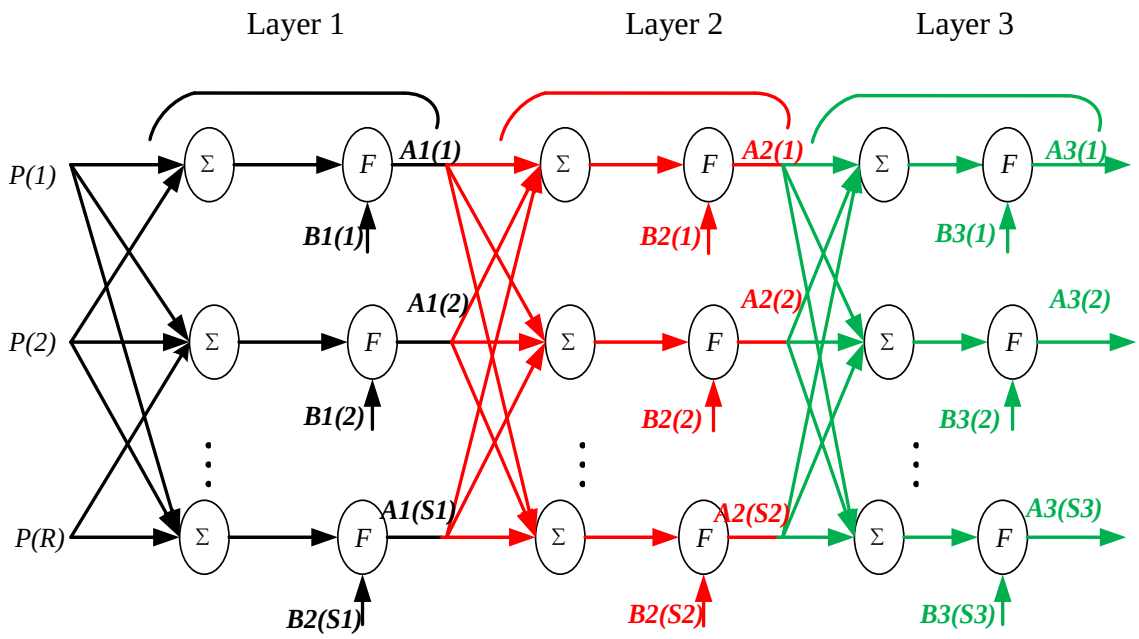

Figure 3-16: A Three-Layer Neural Network.

3.7.3 Back Propagation

Backpropagation was created by generalizing the Widrow-Hoff learning rule to multiple layer networks and nonlinear differentiable transfer functions. Input vector and corresponding output vectors are used to train a network until it can approximate a function, associate the input vectors or classify input vectors in an appropriate way as defined by the user. A very valuable consequence of this definition is that every continuous function is Borel-measurable [38] [39]. Hence every linear or nonlinear continuous function is realizable with a feedforward sigmoidal neural network.

The backpropagation learning rules are used to adjust weights and biases of networks to minimize the sum squared error of the network. this is done by continually changing the values of the network weights and biases in the direction of steepest descent with respect error. This is called a gradient descent procedure. Change in each weight and bias are proportion to the effect of that element on the sum squared error of the network.

Trained backpropagation networks tend to give reasonable answers when presented with inputs that they have never seen, if these inputs are similar to training data. This generalization property makes it possible to train a network on a representative set of input/ target pairs and get good results for new inputs without training the network on all possible input/output pairs (see appendix A).

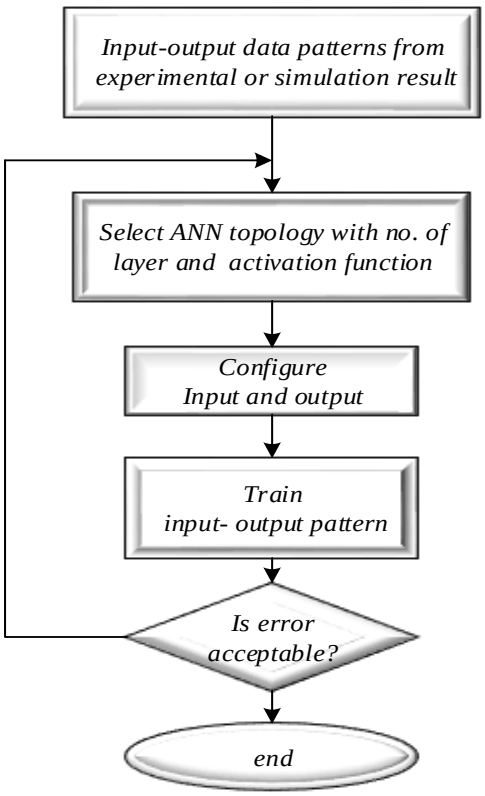

Figure 3-17: Backpropagation training of feedforward neural network flow chart

3.7.4 Neural Network Based Speed Estimator

There are many possibilities of using artificial intelligence based estimators. One can use ANN based speed estimators is described.

ANN speed estimators have the following advantage compare to the others.

- The calculation time can be shorter, because of the parallel processing
- The system can calculate almost correctly, even if the information is not complete (redundancy of the system)
- The ANN can work as low pass filter, so one do not need the additional filters
- The development time of such an estimator is rather short comparing to the others
- The systems based on ANN are robust to parameter variations and noise.

As mentioned before, there are many attempts to solve various estimation problems, such approach is usually not the most effective. Usually we know at least rough mathematical

description of the process to be observed or controlled. Many ANN based estimation will be more effective if we utilize this rough knowledge during the design phase, analyze rotor angular speed estimation using $\underline{v_s}$ and $\underline{i_s}$ with a set of signals obtained from nonlinear transformations of voltages and currents.

$$n_1 = \left|\underline{v_s}\right| = \sqrt{v_{sa}^2 + v_{s\beta}^2} \tag{3.46}$$

$$n_2 = \left|\underline{i_s}\right| = \sqrt{i_{sa}^2 + i_{s\beta}^2} \tag{3.47}$$

$$n_3 = \Re(\underline{v_s}\,\underline{i_s}^*) = i_{sa}v_{sa} + i_{s\beta}v_{s\beta} = \left|\underline{v_s}\right|\left|\underline{i_s}\right|\cos\angle(\underline{v_s},\underline{i_s}) \tag{3.48}$$

$$n_4 = \Im(\underline{v_s}\,\underline{i_s}^*) = i_{sa}v_{s\beta} - i_{s\beta}v_{s\beta} = \left|\underline{v_s}\right|\left|\underline{i_s}\right|\sin\angle(\underline{v_s},i_s) \tag{3.49}$$

$$n_5 = \Re\left(\frac{\underline{v_s}}{\underline{i_s}}\right) = \frac{i_{sa}v_{sa} + i_{s\beta}v_{s\beta}}{i_{sa}^2 + i_{s\beta}^2} = \frac{\left|\underline{v_s}\right|}{\left|\underline{i_s}\right|}\cos\angle(\underline{v_s},i_s) \tag{3.50}$$

$$n_6 = \Im\left(\frac{\underline{v_s}}{\underline{i_s}}\right) = \frac{i_{sa}v_{s\beta} - i_{s\beta}v_{sa}}{i_{sa}^2 + i_{s\beta}^2} = \frac{\left|\underline{v_s}\right|}{\left|\underline{i_s}\right|}\sin\angle(\underline{v_s},i_s) \tag{3.51}$$

$$\omega_m = f(\vec{v_s}, \vec{i_s}) \tag{3.52}$$

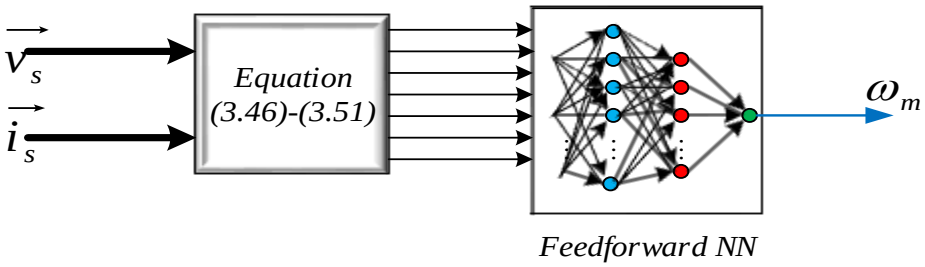

Figure 3-18:ANN Based Speed Estimator

This makes approximation task mush easier, difficult problem is transformed into the well-known one. Moreover, proposed input signals are highly correlated with speed signal. The ANN training process have been speeded up with the help of well-known data mining techniques.

Chapter Four

Simulation Result and Discussion

4.1 Simulink Modeling

The MATLAB/Simulink has used to create, train and test the Simulink models. Simulink has the advantage of being capable of complex dynamic system simulations, graphical environment with visual real time programming and broad selections of tools boxes. Its graphical interface allows selections of functional blocks, their placement on a worksheet, selection of their functional parameters interactive, and description of signal flow by connecting their data lines using a mouse device. Simulink simulates analogue systems and discrete digital systems. It also writes the opportunity of C++ programming, m file and function of MATLAB in to a block to use Simulink environment.

Once the block diagram has been developed it can be simulated using any number of different solvers. These compute the internal state variables of the blocks by solving their respective ordinary differential equations in MTALB modeling configuration parameters. The solver can be significant to decrease the computation time and improve the accuracy of the simulation. The continuous model the state variables has calculated at time of 0.0001sec sampling time.

4.2 NN Based Speed Estimation of IM Simulink Model

The overall MATLAB/SIMULINK model of the Neural Network based speed estimation of induction motor has shown in Figure 4.1. The simulation block includes different sub-functional blocks: the controller blocks, coordinate transformation blocks, the IM modeling blocks, and neural network blocks. The suggested control scheme has simulated in continuous time and most of the blocks used in the design were already available in the standard Simulink library. The detail subsystem would have been seen in the Appendix c.

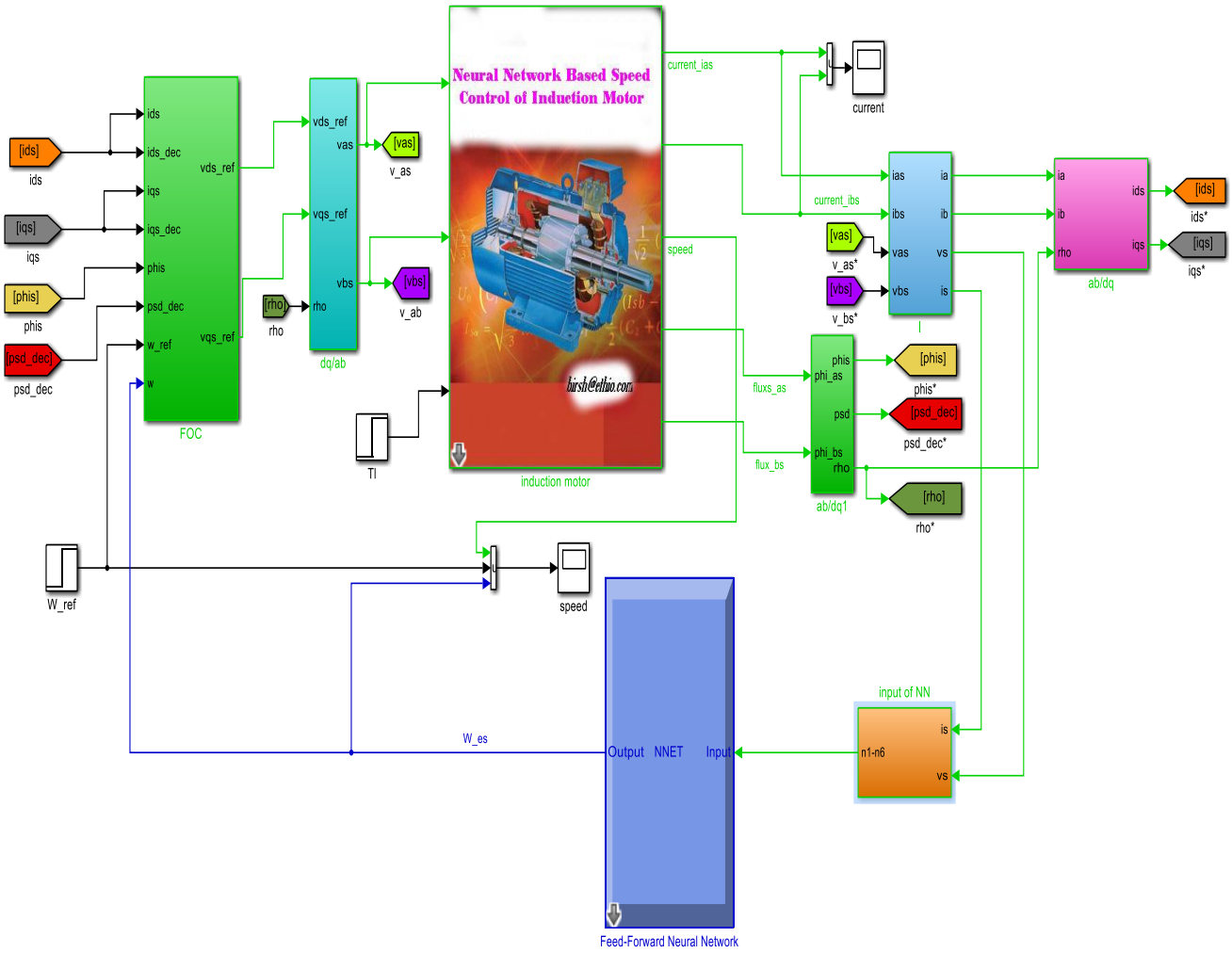

Figure 4-1:Matlab Simulink Model of Induction Motor Speed Estimator Based on NN

4.3 Simulation Results

The simulation result of a NN based speed estimation of induction motor drives was carried out to assess it performance. This simulation results based on the parameters of IM, seen appendix E, the parameter of the IM motor.

The simulation results of NN based speed estimation in express as:

- Transient response
- Variation of parameter (input and motor parameter)

Transient Response

Simulation have been carried out for different operating conditions of the motor drive to study the performance of the NN speed estimator. Frist, the machine has operated at no load. Figure 4.2 shows the reference speed, actual speed, and estimation speed. Due to the instability of estimated speed the initial time shift to 0.5 sec. At 0.5sec the machine was run at 50 rad/s, after one second all most all the reference, actual, and estimated speeds are very quit similar. The maximum overshot of transient response is 5%.

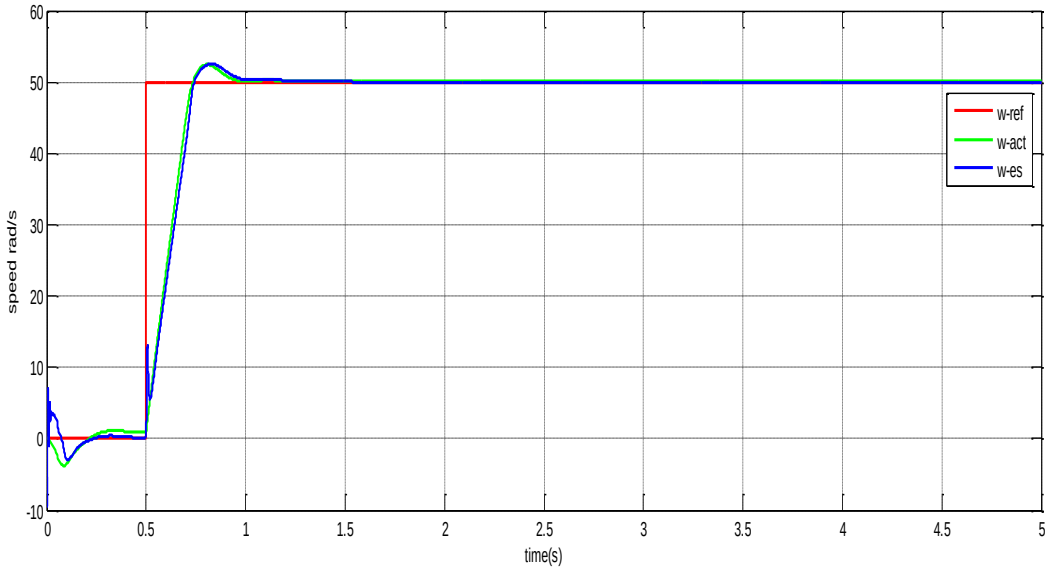

Figure 4-2: Speed Response at no-Load.

There is an error of less than 0.2% in the estimated speed and the actual speed. the error of the estimation has been completely acceptable during no-load condition, in steady states operation (after one second); nothing that the step function or estimated speed normally it may be causes the instability of the systems, shown on Figure 4.3 below.

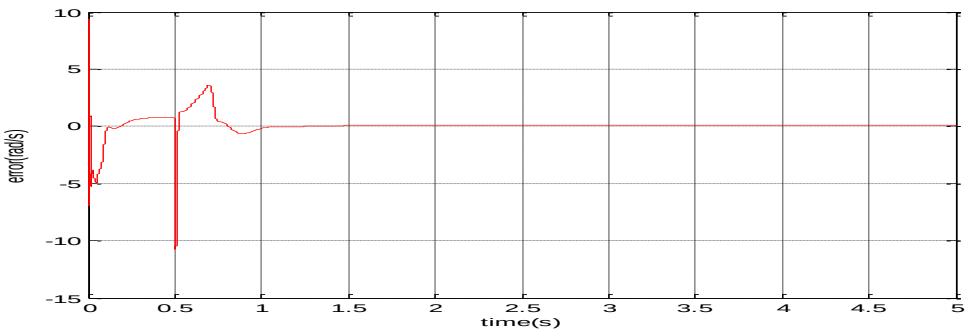

Figure 4-3: Error between actual and estimated speed at no-Load Response

In 0.5 sec the configuration system initially run at 50 rad/s cause distortion of the system, there is an error but the controller governed automatically at one second. The variation of output stator current and devolved torque at no load of induction motor with respect to time are shown below:

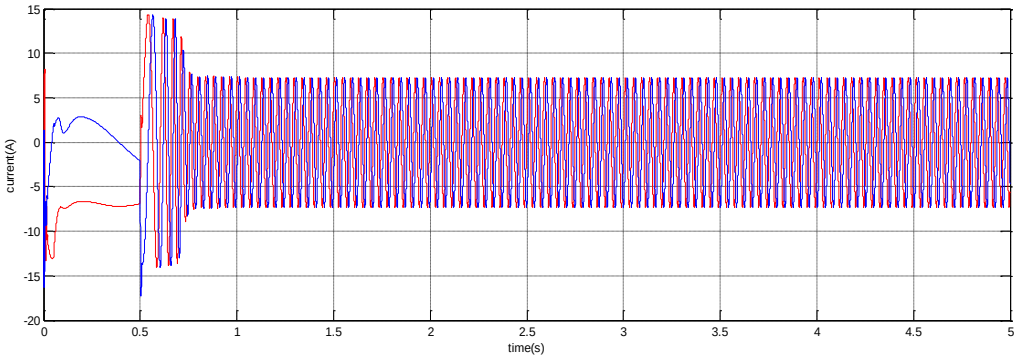

(a)

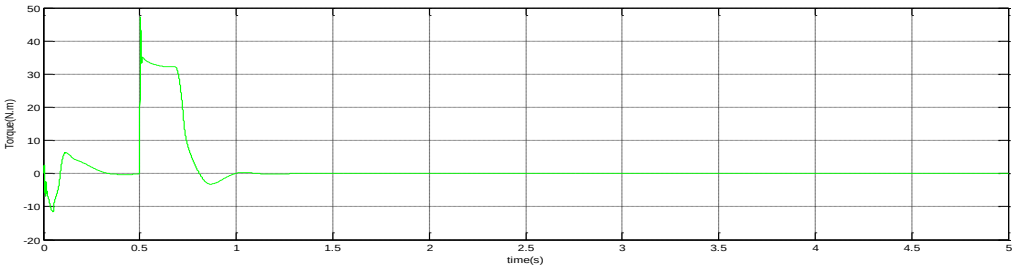

(b)

Figure 4-4:(a) -stator current at no-load condition (b) Developed torque at no-load condition

In the other operation, the performance of the estimator while the machine has loaded and unloaded has studied. The apparatus has first run to 50 rad/s at time of 0.5 sec and then load (5 N.m, No-load, and -5 N.m) has applied at time (2 sec,4 sec and 6 sec).

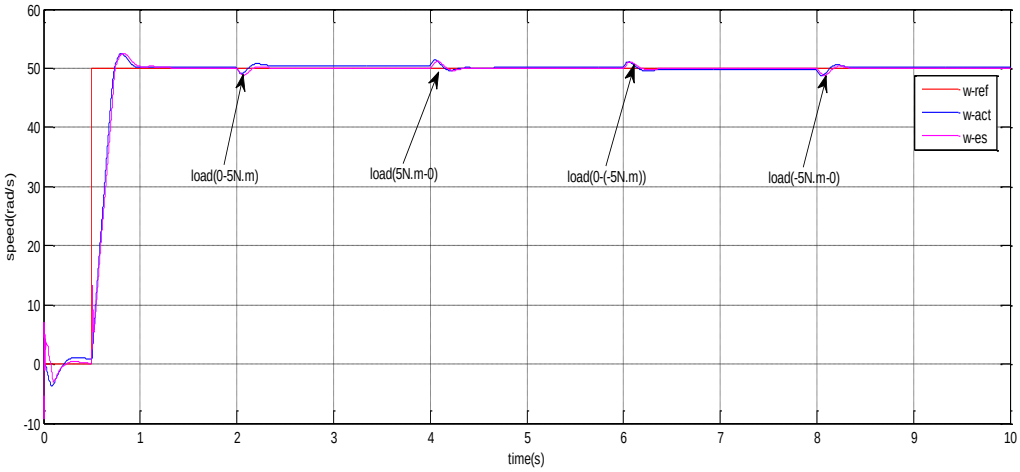

Figure 4-5: Speed Response of due to change Load

Figure 4.6(a) show that the error of estimated speed and actual speed, and the stetted torque when the load torque is change withe the time at the input of sequence satire. It detects that the actual and estimated speed are very well tracks with error has less than 0.74%, and the transient time is very short. The electromechanical torque has shown in Figure 4.6(b), in the time of 0 sec, and 0.5 sec the magnitude of developed torque and error are not stable. This is because of the distortion of initial input start at 0.5 sec or due to estimated speed noise.

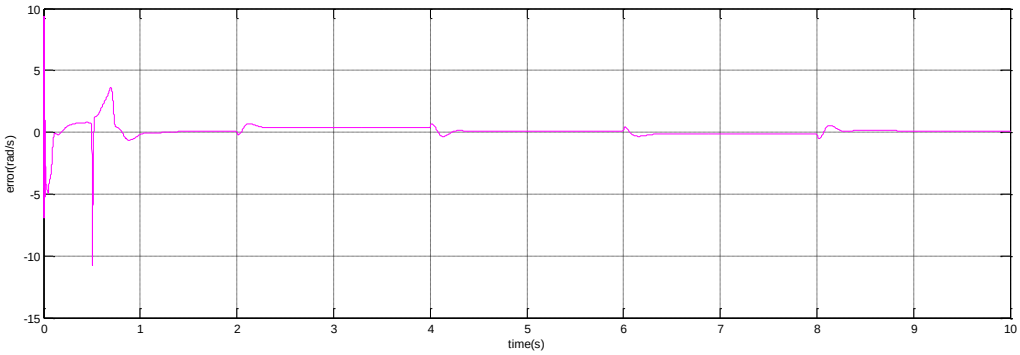

(a)

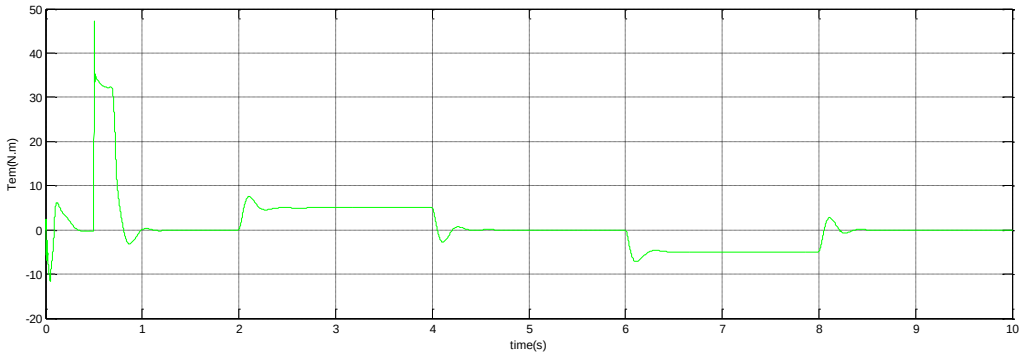

(b)

Figure 4-6:(a) error between actual and estimated speed

(b) devolved torque with change load

Variation of parameter (input and motor parameter)

Variation of input parameter

To illustrate the effectiveness of the high-performance tracking control for induction motor, the proposed neural network estimator was applied to snesorless control the motor drive under variable load torque, and variable reference speed, the performance of speed estimator and speed sensor are evaluated under different operating conditions. Several test cases were completed to evaluate the performances under a variety of operating conditions. However, for the briefness, important results have been reported, this are:

- change the reference speed (repeating sequence stair) as input
- change the load torque (repeating sequence stair) as input
- change both speed and toque (repeating sequence) as input

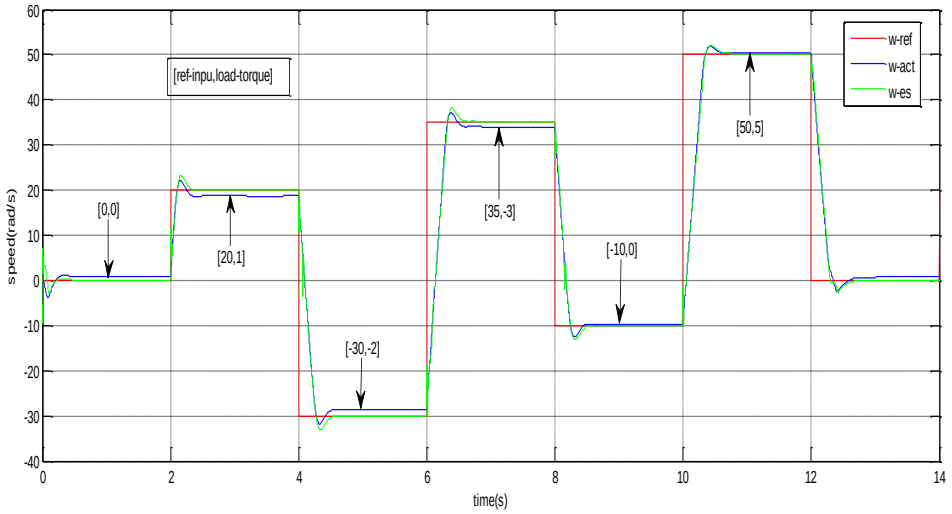

(a)

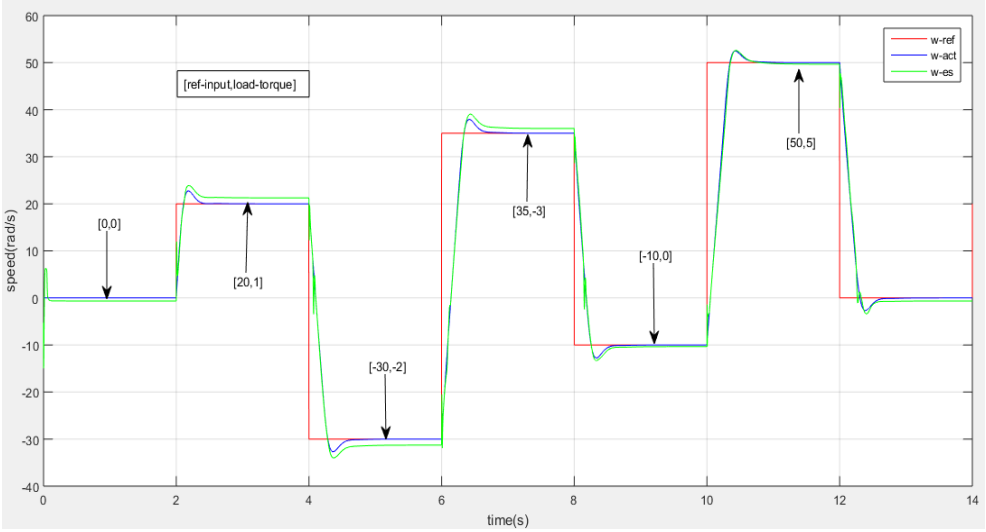

(b)

Figure 4-7:(a):Reference speed and load torque variation response without sensor
(b): Reference speed and load torque variation response with sensor

As shown in Figure 4.7, until t= 2 sec, and time from 12 sec to 14 sec, the reference speed and load torque is zero. At a time of t=2 sec up to 4 sec the reference speed change to 20 rad/s and also at the same time the load torque change to (1 N.m). In addition, the time from 4 sec to 6 sec, 6 sec to 8 sec, 8 sec to 10 sec, and 10 sec to 12 sec both the reference speed

and load torque are vary from (20 to -30, -30 to 35, 35 to -10, and -10 to 50) rad/s and (1 to -2, -2 to -3, -3 to 0, and 0 to 5) N.m respectively.

The result show that the output of the without sensor (speed estimator) and with sensor, which has made against the reference speed and load torque variations, follows the operation of forward and revers directions. More of this, Figure 4.8 shows the result of error (less than 4% between estimated and actual speed without speed sensor, the estimated speed more closed to reference speed), and 6.3% of error between actual and estimated speed with speed sensor. At time of 0 sec, 2 sec, 4 sec, 6 sec, 8 sec, 10 sec, and 12 sec the estimated speed is cause instability due to noise or load variation; then error also variation until reached steady state, this is because of the variation of command speed and load torque, the controller also composite very quickly to reject the disturbance.

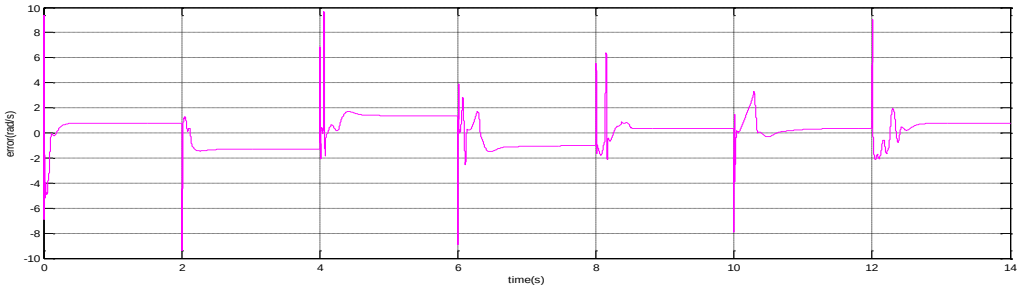

(a)

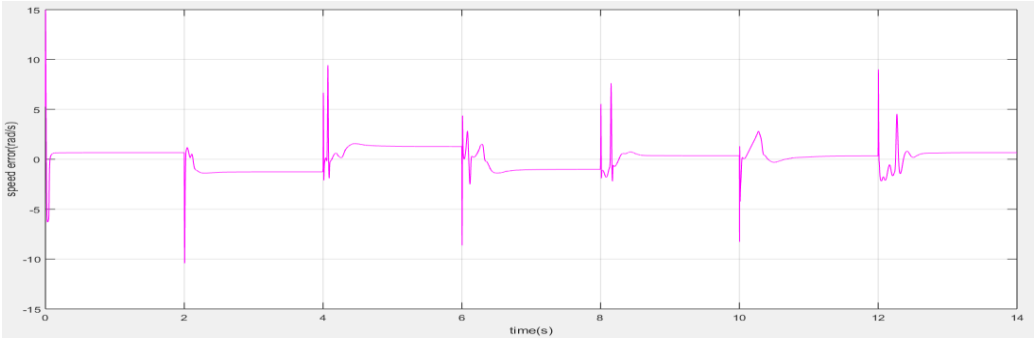

(b)

Figure 4-8:(a) error between actual and estimated speed without sensor
(b) error between actual and estimated speed with sensor

Variation of Motor Parameters

For high dynamic performance of induction machine in different application such as industry, manufacturing, etc., their control remains a challenging problem because they exhibit significant non-linearity's and it is well known that uncertainties of plant parameters and influence of unknown external disturbances can degrade significant the performance of the system.

To show the robustness of the proposed estimator compared with sensor drive, assume that the parameters of the inductance and pole have been nominal values, and it is evident that the speed response of the system is not affected by the variation. Let seen the variation in different case:

- stator resistance variation (100% increase)
- rotor resistance variation (100% increase)

For shortness, only see with 5 N.m external disturbance and the reference speed (0,50,20) rad/s, other parameters of motor are constant.

As it has mentioned the earlier, one of the main problems associated with control of induction machine is the stator winding resistance variation. In practical, the stator resistance changes because of temperature variation caused by machine losses. The resistance variation caused by machine losses could be represented as follows:

$$R_s = R_{so}[1+\alpha(T-T_0)] \tag{4.1}$$

where R_s and R_{so} are the respective actual and initial stator resistance, α is the temperature coefficient of resistance T and T_0 are the actual and initial stator winding temperature respectively. As the resistance value varies by temperature, a mismatch between actual and estimated stator resistance occurs which can be deteriorate the performance of classical controller.

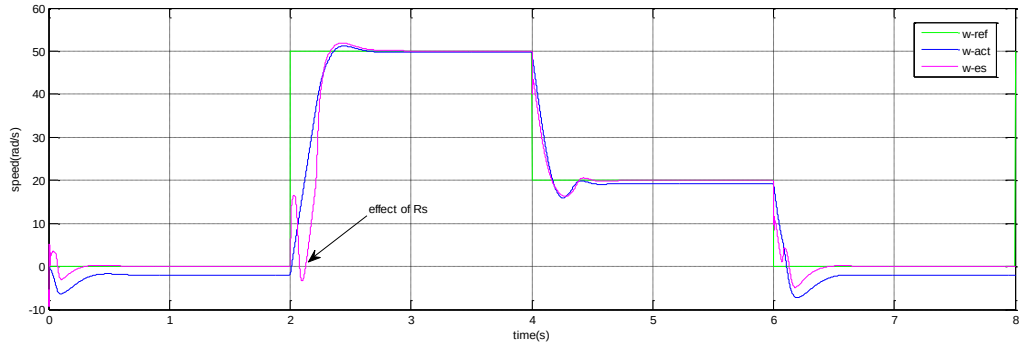

(a)

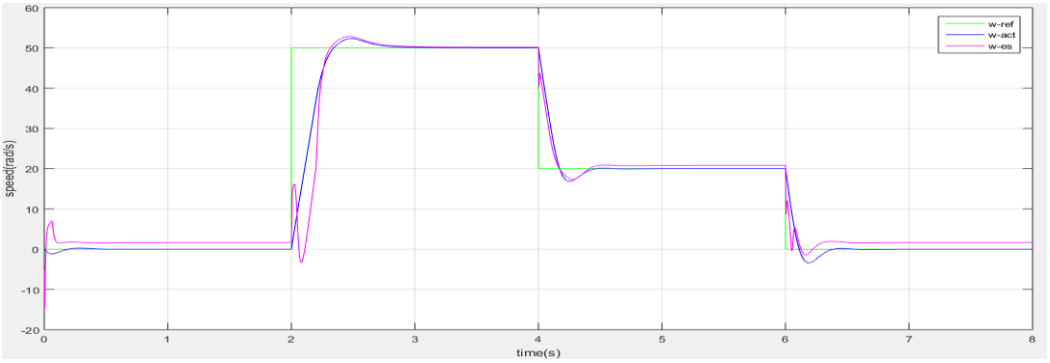

(b)

Figure 4-9:the stator resistance 100% increase (a) without sensor, and (b) with sensor

The simulation results stator resistance variations are shown in Figure 4.9. At first Figure 4.9 (a), the estimated resistance increase by two times actual stator resistance without speed sensor, at step functions of load torque (5N.m) has applied at zero second, and the repeating sequence functions of input speed (0,50,20) rad/s has applied on two second sample time. It could be clearly seen that with such a resistance variation, as describe the earlier, the actual and estimated speed are remained unaffected at steady state. At 0 sec,2 sec,4 sec and 6 sec there is noise due to instability of estimated speed. There are not affect to estimated and actual speed during steady state operation, the error is less than 3.5% (it can be due to input function or estimated speed noise signal), this is an acceptable.

Similar Figure 4.9 (b) show that the estimated stator resistance increase to two times the actual stator resistance with speed sensor, at 2 sec the estimated speed vary compare to actual

speed; this variation come from because the variation of stator resistance. The error between estimated and actual speed are less than 4% due to the actual speed deliver to the controller.

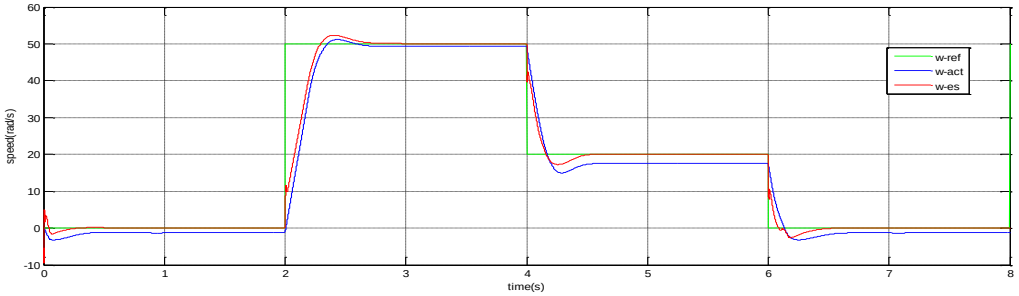

(a)

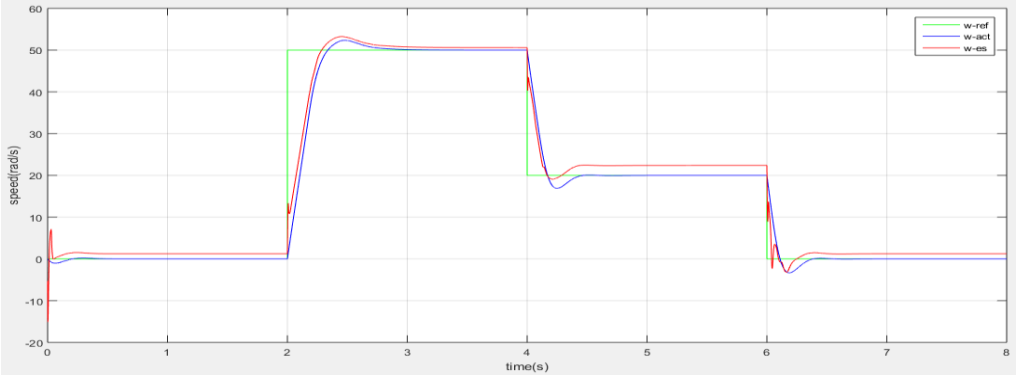

(b)

Figure 4-10: the rotor resistance increase 100% (a) without sensor (b) with sensor

The variation of rotor resistance has a most important issue on the performance of control systems. In the above, Figure 4.10(a) the rotor resistance has increase two time of actual rotor resistance without sensor, and Figure (b) show that the estimated rotor resistance has increase two times the actual speed with the load torque 5N.m and reference input as the function of repeating sequence (0,50,20) rad/s with sample time two second. The performance of the variation rotor resistance has very closed to the variation of stator resistance. So that, the variation of resistance is not affect at steady state operation condition of self-commissioning drive. Because the controller depends on the initial value of plant parameter, not the parameter during operation condition which might change.

Chapter Five

Conclusion and Future Work

5.1 Conclusion

Currently, induction machines have an interesting point for industry, because simplicity maintenance and low cost compere to other but the controller part has very challenging because the nonlinearity and parameter sensitivity. In this thesis, a neural network based speed estimation of induction motor, due to remove the speed sensor. The proposed method where the feedforward neural network has using (multilayer network) three layer, ten neurons for the first layer, five neurons for the second layers and one neurons for output layers with the inputs of stator voltage and current used to provide the estimation of rotor speed.

The simulation results show that, the system has robust enough in a wide range of speed and machine load for steady state in different case, such as no-load, load condition, the variation of the input parameters, change stator and rotor resistance. It was found out that the estimator has been smooth speed tracking and torque response in both forward, reveres operation and low speed operation. There is an error less than 0.25% between actual and estimator speed for input parameter variations (reference speed and load torque), motor parameter variation (stator and rotor resistance change), and also the speed variation error between estimated and actual speed have been less than 4%. The comparison of neural network based speed estimator and induction motor drive with sensor are almost the same.

In general, neural networks are particularly suitable for sensorless control of motor drive applications. It is composed of many highly-interconnected processing elements (neurons) working in unison to solve specific problems. Therefore, the system has independence to the knowledge of some machine parameters or their variation during working. This achievement has considered to be significant impact to without mechanical speed sensor operation of induction motor.

5.2 Future Work

Neural networks have been applied very successfully in the identification and control of dynamic systems. All current NN technologies will most likely be vastly enhanced upon in the future. Everything form handwriting, speech, and image recognitions will become more sophisticated as researchers develop better training methods and network architectures.

In the future, tolerate behinds of drive:

- Different topology of neural network behinds feedforward and learning algorithms
- Application neural network based on robots that can see, feel, and predict, self -driving cars, and self-diagnosis of medical problems.
- The thesis can be also extended for hard ware components based on PLC and FPGA for automations.

Reference:

[1] Stephen J.Chapman, Electric Machinery Fundamentals, Fifth Edition.

[2] Bimal K.Bose, Modern Power Electronics and AC Drives, The university of Tennessee, Knoxvill, 2002.

[3] A. E. Fitzgerald, Electrical Machine, sixth edition, Cambridge, MA March 5, 2002.

[4] C.Mohan,G.Meerimatha and K.kumar,Indirect Vector Control of Induction Motor Using Pi Speed Controller and Neural Networks, Vol.3, Issue.4, Jul - Aug. 2013 pp-1980-1987.

[5] T.Ali,Y.M.Abbas,and A.osman, Control of Induction Motor Drive using Artificial Neural Network, SUST Journal of Engineering and Computer Science (JECS), Vol. 15, No. 2, 2014.

[6] F.Haghoeian, M.A.Ouhrouche and J.S.Thongam, Speed Estimation Using Neural Network in Vector Controlled Induction Motor Drive, Int. Conf. on Dynamic System and Control, Venice, Italy, November 2-4, 2005 (pp592-597).

[7] A.E.Babikar, F.E Rahman, Indirect Field Oriented Control of Induction Motor Drive Using Fuzzy Controller, Journal of Engineering and Computer Science (JECS), Vol. 16, No. 2, 2015.

[8] L.M.Grzesiak,V.Meganck,B.Ufnalski and J.sobolewski,Genetic Algorithm for Parameters Optimization of ANN-based Speed Controller, The International Conference on, 2007.

[9] S.C.Venkatesh, The Development of a Digital Controller for a Three-Phase Induction Motor,M.S.thesis, Massachusetts Institute of Technology,May 1994.

[10] Jogendra Singh Thongam, High Performance Sensorless Induction Motor Drive June2006.

[11] Heath Hofmann, Electric Machinery and Drives, Department of Electrical Engineering and Computer Science, the University of Michigan, 2015.

[12] R.H Park, Two-Reaction Theory of Synchronous Machines, University of Waterloo, Canada, October, 2000

[13] R.J. Lee, P.Pillay and R.G.Harley, D,Q Reference Frames for the Simulation of Induction Motors, Department of Electrical Engineering, University of Natal, South Africa, 1984.

[14] D.W. Novotny and T.A. Lipo, Vector Control and Dynamics of AC Drives, First Edition.

[15] Werner Leonhard, Control of Electrical Drives, Third Edition

[16] Popescu M., Induction Motor Modelling for Vector Control Purposes, Helsinki University of Technology, Laboratory of Electro mechanics, Report, Espoo 2000, 144 p.

[17] Dal Y.Ohm, Dynamic Model of Induction Motors For Vector Control, Drivetech, Inc., Blacksburg, Virginia.

[18] Zelmira Ferkova, Comparison of Two-Phase Induction Motor Modeling in ANSYS Maxwell 2D and 3D Program, Technical University of Kosice Kosice, Slovakia.

[19] Sifat Shah, A. Rashid, MKL Bhatti, Direct Quadrate (D-Q) Modeling of 3-Phase Induction Motor Using MatLab / Simulink, COMSATS Institute of Information and Technology, Abbottabad, Pakistan.

[20] Tze-Fun Chan and Keli Shi, Applied Intelligent Control of Induction Motor Drives, First Edition,2011.

[21] P.C.Karuse, Analysis of Electrical Machinery and Drive Systems, Second Edition.
[22] M.G.Say, Alternating current Machines, Fourth Edition, Heriot-watt University, Edinburgh.
[23] Bimal K. Bose, Power Electronics and Motor Drives, Advances and Trends, University of Tennessee Knoxville, Tennessee, 2006.
[24] Richard C.Dorf, Robert H.Bishop, Modern Control Systems, Twelfth Edition, 2011.
[25] Rik W. De Doncker, and Donald W. Novotny, The Universal Field Oriented Controller, IEEE Transactions On Industry Applications, Vol. 30, No. 1, 1994.
[26] Joachim Holtz, Sensorless Control of Induction Motor Drives, Proceedings of The IEEE, Vol. 90, No. 8, August 2002.
[27] A. Larabi, M.S. Boucherit, Speed Sensorless Control of Induction Motor Using Model Reference Adaptive System, Process Control Laboratory, Algiers, Algeria.
[28] A. Larabi, MO. Mahmoudi, M.S. Boucherit, Speed Sonsorless Vector Control of Induction Motor Using Adaptive Model Reference Method, International Symposium on Power Electronics, Electrical Drives, Automation and Motion, 2008.
[29] R. Gunabalan, V. Subbiah, and B. Rami Reddy, Sensorless Control of Induction Motor with Extended Kalman Filter on TMS320F2812 Processor, International Journal of Recent Trends in Engineering, Vol 2, No. 5, November 2009.
[30] Young-Real Kim, Seung-Ki Sul, and Min-Ho Park, Speed Sensorless Vector Control of Induction Motor Using Extended Kalman Filter, IEEE Transactions on Industry Applications, VOL. 30, NO. 5, 1994.
[31] Yang Wenqiang, Cai Xu, Jiang Jianguo, Speed Sensorless Vector Control of Induction Motor Based On Reduced Order Extended Kalman Filter, Shanghai Jiaotong University Shanghai P.R.China.
[32] Nicolae Patrascoiu, Adrian Tomus, Design of an extended Luenberger observer for sensorless vector control of induction machines using virtual instrument, Automatics, Computers, Electrical and energetics Engineering University of Petrosani, Romania.
[33] Lech M.Grzesiak, Bartłomiej Ufnalski, Designof Speed Estimator for Induction Motor using Principal Component Analysis and Neural Networks. Politechnika Warszawska, Instytut Sterowania i Elektroniki Przemysłowej.
[34] T. Pană and O. Stoicuţa, Design of an Extended Luenberger Observer for Sensorless Vector Control of Induction Machines under Regenerating Mode. 12th International Conference on Optimization of Electrical and Electronic Equipment, 2010.
[35] Bimal K. Bose, Neural Network Applications in Power Electronics and Motor Drives-An Introduction and Perspective, IEEE Transactions On Industrial Electronics, Vol. 54, No. 1, 2007.
[36] M. Cuibus, V. Bostan; S. Ambrosii, C. Ilas, R. Magureanu, Luenberger, Kalman and Neural Network Observers for Sensorless Induction Motor Control, Politechnical University of Bucharest, Romania.

[37] Teresa Orlowska-Kowalska, Czeslaw T.Kowalski, Neural Network Application for Flux and Speed Estimation in the Sensorless Induction Motor Drive, Institute of Electric Machines and Drives, Technical University of Wroclaw, Poland.

[38] Dariusz L. Sobczuk, Application of ANN for Control of PWM Inverter Fed Induction Motor Drives, Warsaw University of Technology Faculty of Electrical Engineering. 1999.

[39] Bart Kosko, Neural Networks and Fuzzy Systems a Dynamical Systems Approach to Machine Intelligence, University of Southern California.

[40] Fang-Zheng Peng, and Tadashi Fukao, Robust Speed Identification for Speed-Sensorless Vector Control of Induction Motors, IEEE Transactions On Industry Applications, Vol. 30, No. 5, September / October 1994.

[41] Seong-Hwan Kim, Tae-Sik Park, and Gwi-Tae Park, Speed-Sensorless Vector Control of an Induction Motor Using Neural Network Speed Estimation. IEEE Transactions on Industrial Electronics, Vol. 48, No. 3, June 2001.

[42] Xingyi Xu Rik De Doncker and Donald W. Novomy, A Stator Flux Oriented Induction Machine Drive, Dept. of Electrical and Computer Engineering, Univ. of Wisconsin-Madison Madison, U.S.A.

Appendix

A: Backpropagation

The generalized multilayer layer neural network, calculation of weight for output layer, with the neuron *m*, *n* number of layer, and derive a mathematical expression for the iteration of its input weight $W_{lm.n}$, which receives signal $F_{l.n-1}$ from neuron *l*. The output of neuron *m*, $F_{m.n}$ is compared with the desired or target value D_m to calculate the error ξ_m as:

$$\xi_m = D_m - Y_m \tag{A.1}$$

Where $Y_m = F_{m.n}$; the objective function to be minimized is defined as:

$$\xi_m{}^2 = (D_m - F_{m.n})^2 \tag{A.2}$$

The output $F_{m.n}$ and the corresponding ξ_m^2 will vary with the variation of weight $W_{lm.n}$, with all the input signals remaining constant. To minimize ξ_m^2 by the gradient method, the change in weight must be proportional to the rate of change of the square error with respect to that weight, that is:

$$\Delta W_{lm.n} = -\eta \frac{\partial \xi_m^2}{\partial W_{lm.n}} \tag{A.3}$$

Where η is the constant of proportionality defined as the learning rate. Therefore, the new weight is given as:

$$W_{lm.n}(k+1) = W_{lm.n}(k) + \Delta W_{lm.n} \tag{A.4}$$

$$= W_{lm.n}(k) - \eta \frac{\partial \xi_m^2}{\partial W_{lm.n}} \tag{A.5}$$

Where $W_{lm.n}(k) =$ old weight and *k*=number of iterations involved. The partial derivative in Equation (A.3) can be evaluated by the chain rule of differentiation as follows:

$$\frac{\partial \xi_m^2}{\partial W_{lm.n}} = \frac{\partial \xi_m^2}{\partial F_{m.n}} \cdot \frac{\partial F_{m.n}}{\partial A_{m.n}} \cdot \frac{\partial A_{m.n}}{\partial W_{lm.n}} \tag{A.6}$$

Where each term can be evaluated individually. The first term follows from Equation (A.2);

$$\frac{\partial \xi_m^2}{\partial F_{m.n}} = -2(D_m - F_{m.n}) = -2\xi_m \tag{A.7}$$

The second term follows the differentiation of the sigmoidal function (see Figure 3.13(c)) for simplicity, which can be derives in the form;

$$\frac{\partial F_{m.n}}{\partial A_{m.n}} = \frac{\partial}{\partial A_{m.n}}\left(\frac{1}{1+e^{-A_{m.n}}}\right) = F_{m.n}(1-F_{m.n}) \tag{A.8}$$

Since the signal $A_{m.n}$ is contributed by all the input signals of the neuron *m*, we can write

$$A_{m.n} = \sum_{l=1}^{P} W_{lm.n} . F_{l.n-1} \tag{A.9}$$

Where $p =$ number of neurons in the middle layer. Taking its partial derivative with respect to $W_{lm.n}$ gives

$$\frac{\partial A_{m.n}}{\partial W_{lm.n}} = F_{l.n-1} \tag{A.10}$$

Which indicates that only $F_{l.n-1}$ contributes to the change in output when $W_{lm.n}$ is changed. Combining Equations (A.6) -(A.10) we get

$$\frac{\partial \xi_m^2}{\partial W_{lm.n}} = -2(D_m - F_{m.n})F_{m.n}(1-F_{m.n})F_{l.n-1} \tag{A.11}$$

$$= \delta_{lm.n-1} F_{l.n-1} \tag{A.12}$$

or $$\Delta W_{lm.n} = \eta \delta_{lm.n} F_{l.n-1} \tag{A.13}$$

$$\text{where} \quad \delta_{lm.n} = 2(D_m - F_{m.n})F_{m.n}(1 - F_{m.n}) = 2\xi_m \frac{\partial F_{m.3}}{\partial A_{m.n}} \tag{A.13}$$

one of the problems in gradient descent weight optimization is the local (or false) minimum instead of the global minimum point 0. The operation may be locked at this point, giving a false ξ_m^2 minimization effect. To jump across this ditch, a momentum term is added on the right of Equation (A.5) which is given as follows:

$$W_{lm.n}(k+1) = W_{lm.n}(k) - \eta \frac{\partial \xi_m^2}{\partial W_{lm.n}} + \mu\left[W_{lm.n}(k) - W_{lm.n}(k-1)\right] \tag{A.14}$$

where μ - momentum factor.

B: Decupling control

For decoupling control, we can now make a derivation of control equations of indirect vector control with the help of *d-q* equivalent circuits (Figure 2-5). The rotor circuit equations can be written as:

$$\frac{d\phi_{rd}}{dt} + R_r i_{rd} - (\omega_e - \omega_r)\phi_{rq} = 0 \tag{B.1}$$

$$\frac{d\phi_{rq}}{dt} + R_r i_{rq} + (\omega_e - \omega_r)\phi_{rd} = 0 \tag{B.2}$$

The rotor flux linkage expression can be given as:

$$\phi_{rd} = L_r i_{rd} + L_m i_{sd} \tag{B.3}$$

$$\phi_{rq} = L_r i_{rq} + L_m i_{sq} \tag{B.4}$$

From the above equations, we can write

$$i_{rd} = \frac{1}{L_r}\phi_{rd} - \frac{L_m}{L_r} i_{sd} \tag{B.5}$$

$$i_{rq} = \frac{1}{L_r}\phi_{rq} - \frac{L_m}{L_r} i_{sq} \tag{B.6}$$

The rotor currents in Equation (B.1) and (B.2), which are inaccessible, can be eliminated with the help of Equation (B.5) and (B.6) as

$$\frac{d\phi_{rd}}{dt} + \frac{R_r}{L_r}\phi_{rd} - \frac{L_m}{L_r} R_r i_{sd} - \omega_{sl}\phi_{rq} = 0 \tag{B.7}$$

$$\frac{d\phi_{rq}}{dt} + \frac{R_r}{L_r}\phi_{rq} - \frac{L_m}{L_r} R_r i_{sq} + \omega_{sl}\phi_{rd} = 0 \tag{B.8}$$

Where $\omega_{sl} = \omega_e - \omega_r$ has been substituted,. Multiplying Equation(B.7) and(B.8) by $T_r = \frac{L_r}{R_r}$ we gat

$$(1+pT_r)\phi_{rd} - L_m i_{sd} - T_r \omega_{sl}\phi_{rq} = 0 \quad \text{(B.9)}$$

$$(1+pT_r)\phi_{rq} - L_m i_{sq} + T_r \omega_{sl}\phi_{rd} = 0 \quad \text{(B.10)}$$

In these equation, ϕ_{rd} and ϕ_{rq} are to be eliminated and replaced by ϕ_{sd} and ϕ_{sq}. The stator flux expression can be written from *d-q* equivalent circuits as

$$\phi_{sd} = L_s i_{sd} + L_m i_{rd} \quad \text{(B.10)}$$

$$\phi_{sq} = L_s i_{sq} + L_m i_{rq} \quad \text{(B.11)}$$

$$\text{or } i_{rd} = \frac{\phi_{sd}}{L_m} - \frac{L_s}{L_m} i_{sd} \quad \text{(B.12)}$$

$$i_{rq} = \frac{\phi_{sq}}{L_m} - \frac{L_s}{L_m} i_{sq} \quad \text{(B.13)}$$

Substituting Equations (B.12) and (B.13) in to Equation (B.3) and (B.4) respectively we get

$$\phi_{rd} = \frac{L_r}{L_m}\phi_{sd} + (L_m - \frac{L_r L_s}{L_m})i_{sd} \quad \text{(B.14)}$$

$$\phi_{rq} = \frac{L_r}{L_m}\phi_{sq} + (L_m - \frac{L_r L_s}{L_m})i_{sq} \quad \text{(B.15)}$$

These equations relate stator and rotor fluxes with stator currents. Substituting Equations (B.14) and (B.15) in Equations (B.9) and (B.10) respectively, then multiplying both side by L_m / L_r, and simplifying, we get

$$(1+pT_r)\phi_{sd} = (1+\sigma pT_r)L_s i_{sd} + \omega_{sl} T_r(\phi_{sq} - \sigma L_s i_{sq}) \quad \text{(B.16)}$$

$$(1+pT_r)\phi_{sq} = (1+\sigma pT_r)L_s i_{sq} - \omega_{sl}T_r(\phi_{sd} - \sigma L_s i_{sd}) \quad \text{(B.17)}$$

Where $\sigma = 1 - L_m^2 / L_s L_r$; for decoupling control, it is desirable that $\phi_{sq} = 0$, therefore:

$$(1+pT_r)\phi_{sd} = (1+\sigma pT_r)L_s i_{sd} - \sigma L_s T_r \omega_{sl} i_{sq}) \quad \text{(B.18)}$$

$$(1+\sigma pT_r)L_s i_{sq} = \omega_{sl}T_r(\phi_{sd} - \sigma L_s i_{sd}) \quad \text{(B.19)}$$

From (B.19) an expression to determine the slip frequency is:

$$\omega_{sl} = \frac{(1+\sigma T_r p)L_s i_{sq}}{T_r(\phi_{sd} - \sigma L_s i_{sd})} \quad \text{(B.20)}$$

In order to decouple ϕ_{sd} from i_{sq}, it is required that:

$$\phi_{sd} = \frac{(1+\sigma T_r p)L_s}{(1+T_r p)}\left(i_{sd} - \frac{\sigma T_r \omega_{sl}}{(1+\sigma T_r p)} i_{sq}\right) \quad \text{(B.21)}$$

$$\text{From this, } i_{dq} = \frac{\sigma T_r \omega_{sl}}{(1+\sigma T_r p)} i_{sq} \quad \text{(B.22)}$$

Substituting ω_{sl} in to (B.22)

$$i_{dq} = \frac{\sigma L_s}{(\phi_{sd} - \sigma L_s i_{sd})} i_{sq}^2 \quad \text{(B.23)}$$

Where, $p = \frac{d}{dt}$ denotes the differential operator and $T_r = \frac{L_r}{R_r}$ is the rotor time constant

C: Block diagram of Figure 4.1

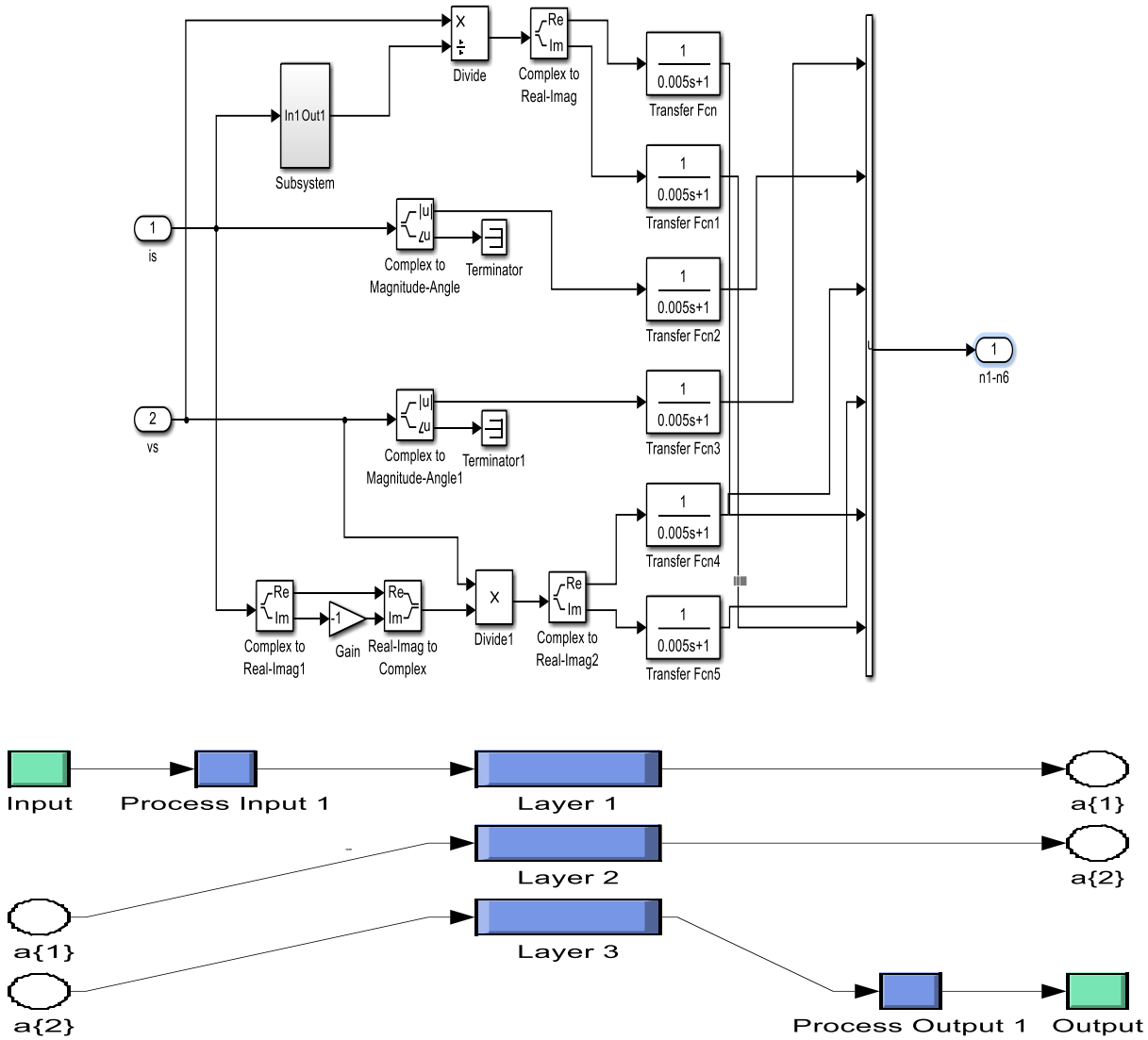

Figure C.1: input of and genism model of NN

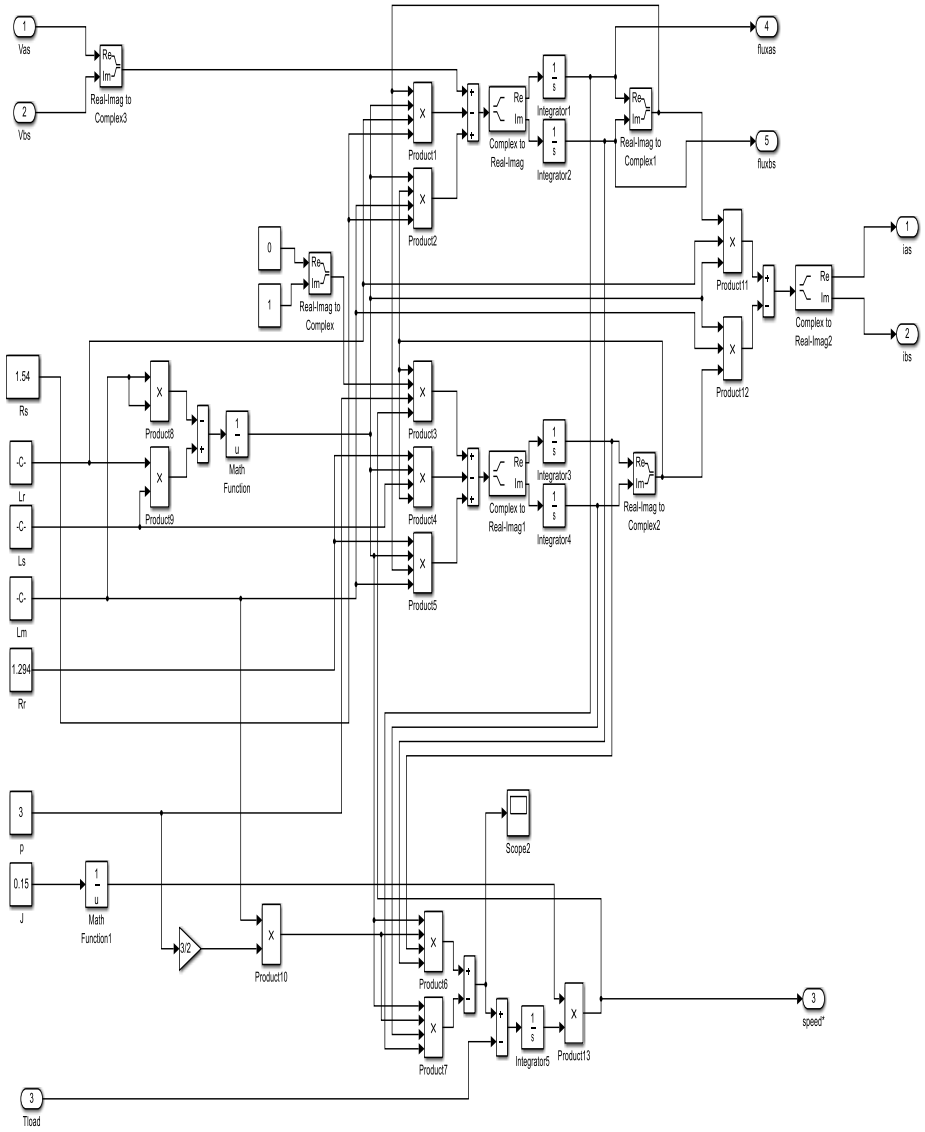

Figure C.2: Stationary reference frame IM MATLAB model

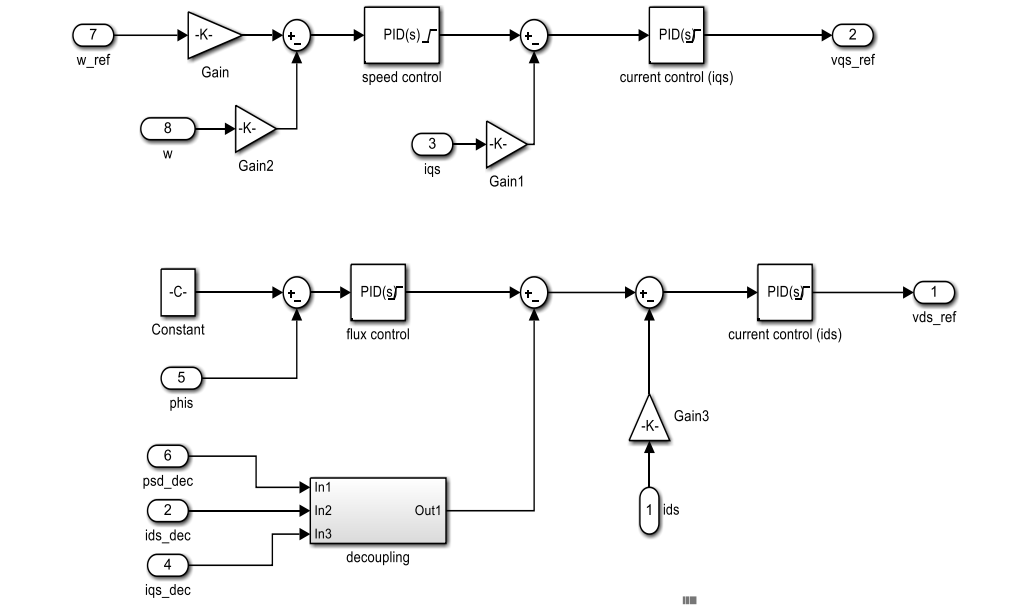

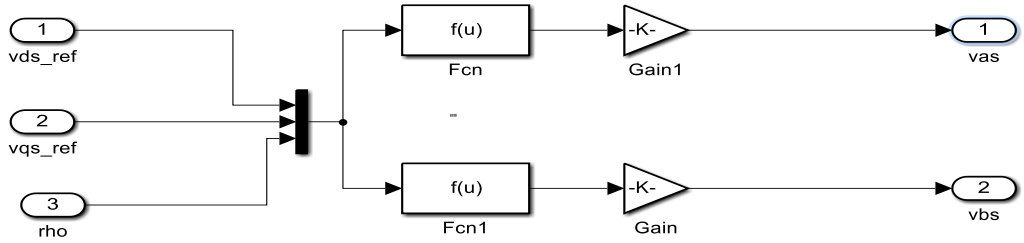

Figure C.3: Vector control and inverse of Park Transformation

D: MATLAB Code of Feedforward Neural Network

```
%Artificial Neural Network for Speed Estimation of Induction Motor
clear all
smodel = 'induction_ann'; %neural network based speed estimator of
%induction motor MATHLAB Simulink file name
open(smodel);
%motor parameter initialization
stator_inductance = 0.1004;
rotor_inductance = 0.0969;
mutual_inductance = 0.0915;
stator_resistance=1.594;
J=0.15; %viscosity constant
P=3; %pole pairs
alpha = 1-((mutual_inductance)^2)/(rotor_inductance*stator_inductance);
rotor_resistance = 1.294;
Tr = rotor_inductance/rotor_resistance;
Ts=0.0001; %sampling time
%PI speed control
ki_w = 120; %speed control of integration gain
kp_w = 8;%speed control of proportional gain
%PI stator flux control
kp_pi = 15; %stator flux control of proportional gain
ki_pi = 50; %stator flux control of integration gain
%PI stator current control (isq)
ki_iqs =5; % integration gain
kp_iqs = 1; % proportional gain
%PI stator current control (isd)
kp_ids = 1; %proportion gain
ki_ids = 5; %integration gain
%%%%%%%%%%%%%%%%%%%%%%%%%%%%%
%Artificial neural network (Feedforward Neural Network)
%10:5:1 structure of multilayer FFNN
%feedforward neural network training
%for speed estimation
es=bg1'; %estimator speed file name training data
mo=bg'; %actual speed file name training data
net = feedforwardnet([10 5]); %10 neuron_input layer; 5 neuron_hidden layer
%and 1 neuron_ output FFNN
%net = layrecnet(1:2,[10 5]);Recurrent Neural Network
%net = elmannet(1:2,[10 5]);Elman Neural Network
net.layers{1}.transferFcn = 'tansig';%input layer activation transfer
%function
net.layers{2}.transferFcn = 'tansig';%hidden layer activation transfer
%function
net.layers{3}.transferFcn = 'purelin';%output layer activation transfer
%function
net.divideFcn='dividetrain';
net = configure(net,es,mo);
net = init(net);
net.trainParam.min_grad = 1e-10;
net.trainParam.epochs = 400;
```

```
disp('Speed Estimation training net...');
net = train(net,es,mo);
%figure plotting
annfig = figure (1);
set(annfig,'units','centimeters','position',[5 5 10 10]);
plot(mo,'r-','Linewidth',1.5);
hold on
grid;
title('speed estimation of induction motor using ann');
xlabel('sample number');
ylabel('velocity [rad/s] ');
y2 = sim(net,es);
plot(y2,'b:','Linewidth',1.5);
hold off;
legend('actual speed', 'estimated speed');
axis([0 5000 -100 100]);
%%%%%%%%%%%%%%%%%%%%%%%%
gensim(net,-1);%Simulink model of FFNN

%ABC_DQ transformation using NN
%or Clark transformation
sim('ABC_DQ_NN1') %file name of MATLAB Simulink of Equation (2.6)
in=sim1'; %input data training file name
out=sim2'; %output data training file name
net = feedforwardnet(4); %4 neuron_input layer; and 6 neuron_ output FFNN
%net = layrecnet(1:2,4);Recurrent Neural Network
%net = elmannet(1:2,4);Elman Neural Network
net.layers{1}.transferFcn = 'tansig';%input layer activation transfer
%function
net.layers{2}.transferFcn = 'purelin';%output layer activation transfer
%function
net.divideFcn='dividetrain';
net = configure(net,in,out);
net = init(net);
net.trainParam.min_grad = 1e-10;
net.trainParam.epochs = 500;
disp('Clark transformation training net...');
net = train(net,in,out);
%%%%%%%%%%%%%%%%%%%%%%%%
gensim(net,-1); % Simulink model of Feedforward Neural Network
```

E: Induction motor parameters and nntraintool

Parameter	Symbol	Unit	Value
Type of rotor	-	-	Squirrel-cage
Number of pole pairs	P	-	*3*
Stator resistance	R_s	Ω	*1.54*
Stator inductance	L_s	*mH*	*100.4*
Rotor resistance	R_r	Ω	*1.29*
Rotor inductance	L_r	*mH*	*96.9*
Mutual inductance	L_m	*mH*	*91.5*
Moment of inertia	J	kgm^2	*0.15*
Rated voltage	V_r	*V*	*220*
Rated speed	ω_r	*rad/s*	*97*
Rated power	P_r	*kW*	*1.5*

Table E.1: Induction Motor nameplate

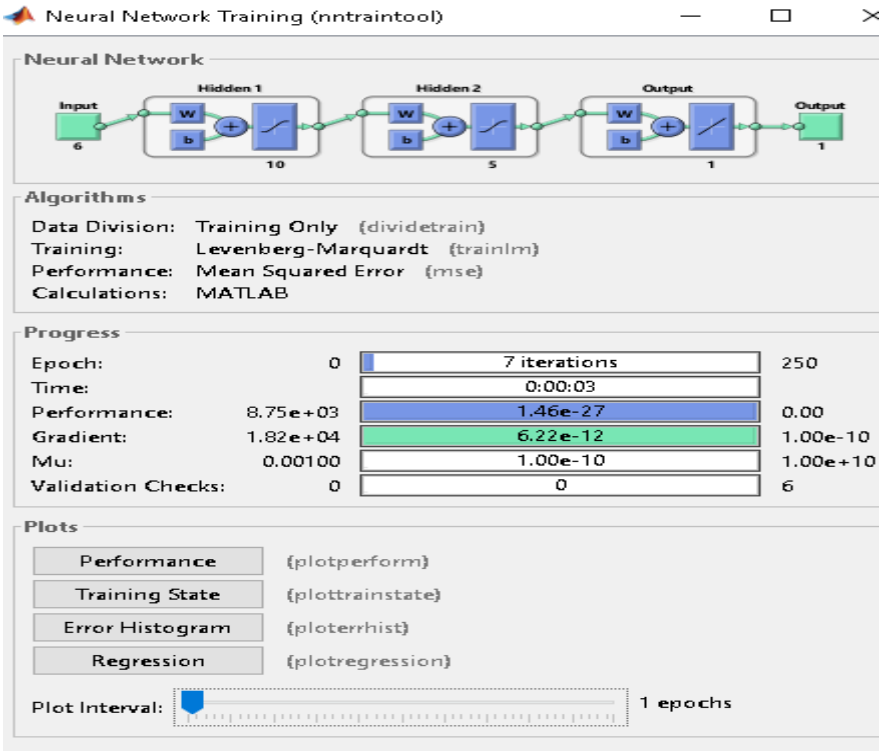

Figure E.1: Neural Network Training Front Page